

©Copyright 2016

Benjamin Janicki

# Design of a Pneumatic Tool for Manual Drilling Operations in Confined Spaces

Benjamin Janicki

A thesis submitted  
in partial fulfillment of the  
requirements for the degree of

Master of Science In Mechanical Engineering

University of Washington

2016

Reading Committee:

Joseph Garbini, Chair

Santosh Devasia, Chair

James Buttrick

Program Authorized to Offer Degree:  
Mechanical Engineering

University of Washington

**Abstract**

Design of a Pneumatic Tool for Manual Drilling Operations in Confined Spaces

Benjamin Janicki

Co-Chairs of the Supervisory Committee:

Professor Joseph Garbini  
Mechanical Engineering

Professor Santosh Devasia  
Mechanical Engineering

This master's thesis describes the design process and testing results for a pneumatically actuated, manually-operated tool for confined space drilling operations.

The purpose of this device is to back-drill pilot holes inside a commercial airplane wing. It is lightweight, and a "locator pin" enables the operator to align the drill over a pilot hole. A suction pad stabilizes the system, and an air motor and flexible drive shaft power the drill.

Two testing procedures were performed to determine the practicality of this prototype.

The first was the "offset drill test", which qualified the exit hole position error due to an initial position error relative to the original pilot hole. The results displayed a linear relationship, and it was determined that position errors of less than .060" would prevent the need for rework, with errors of up to .030" considered acceptable.

For the second test, a series of holes were drilled with the pneumatic tool and analyzed for position error, diameter range, and cycle time. The position errors and hole diameter range were within the allowed tolerances. The average cycle time was 45 seconds, 73 percent of which was for drilling the hole, and 27 percent of which was for positioning the device.

Recommended improvements are discussed in the conclusion, and include a more durable flexible drive shaft, a damper for drill feed control, and a more stable locator pin.

# TABLE OF CONTENTS

	Page
List of Figures . . . . .	iii
Glossary . . . . .	vi
Chapter 1: Introduction . . . . .	1
1.1 Research Question . . . . .	1
1.2 Thesis Statement . . . . .	2
Chapter 2: Background . . . . .	3
2.1 Research Motivation . . . . .	3
2.2 Assembly Environment . . . . .	3
2.3 Back-Drilling . . . . .	6
2.4 Literature Review . . . . .	8
Chapter 3: Design Process . . . . .	11
3.1 Design Approach . . . . .	11
3.2 Design Constraints . . . . .	12
3.3 Preliminary Design Process . . . . .	15
3.4 Five-Axis Stationary Platform . . . . .	21
3.5 Manually Operated Pneumatic Tool . . . . .	25
Chapter 4: Prototype Testing . . . . .	34
4.1 Test Bench . . . . .	34
4.2 Offset Drill Test . . . . .	35
4.3 Prototype Testing . . . . .	40
Chapter 5: Evaluation . . . . .	42
5.1 Offset Drill Test Results . . . . .	42

5.2	Prototype Test Results . . . . .	44
Chapter 6:	Conclusions . . . . .	46
6.1	Discussion of Results . . . . .	46
6.2	Implications of Research . . . . .	48
6.3	Future Design Improvements . . . . .	51
Bibliography	. . . . .	56
Appendix A:	Additional Figures and Tables . . . . .	57
A.1	Matlab Code and Graphs . . . . .	57
A.2	Wing Bay Analysis . . . . .	57
A.3	Preliminary Design Analysis . . . . .	57

## LIST OF FIGURES

Figure Number	Page
2.1 A Boeing 737, which is in the general size range of the airplanes considered in this research. [1] . . . . .	4
2.2 An early design of a tracked crawler with folding arms. . . . .	4
2.3 The cross section of a typical wing bay. . . . .	5
2.4 The view of a typical wing bay as seen from above. Note the access hole and the placements of marks signifying hole locations on the spar chord flanges at each end. . . . .	6
2.5 This figure illustrates the back-drilling procedure. The purpose is to extend an initial pilot hole on the interior of the wing to the exterior of the wing, as shown in (a). This exterior pilot hole will provide the location for the final drill procedure, which will be completed with a larger drill bit from the outside of the wing as shown in (b). . . . .	7
3.1 The wing model as seen from above, with the wing bays labeled by number.	11
3.2 A closer image of the wing bays from above. Several notable features are labeled, such as the access hole and spar chord flanges. . . . .	13
3.3 This graph illustrates that the wing bay height rapidly decreases as the end of the wing is approached. See the appendix for similar graphs. . . . .	14
3.4 This is the Pugh Chart that was analyzed for the stabilization system. See the appendix for similar charts of other systems. . . . .	19
3.5 An early design mockup of how the platform system might fit within a typical wing bay. . . . .	22
3.6 The CAD design of the platform design. . . . .	23
3.7 The final design of the platform system. . . . .	24
3.8 The above figures display the CAD design in Solidworks of the manually operated pneumatic tool. Note that the “locator pin” swings out of the path of the drill bit during drilling. . . . .	26
3.9 The completed prototype for the manually operated pneumatic tool. . . . .	27

3.10	The manually operated pneumatic tool including the air motor, flexible drive shaft, and air supply system. . . . .	28
3.11	The alignment device. . . . .	30
3.12	The manually operated pneumatic tool drill system being aligned with the alignment device. . . . .	31
3.13	The manually operated pneumatic tool being placed in the cross-section of an actual airplane wing. Note that a wedge would be inserted between the handle and the last stringer it spans. . . . .	32
4.1	The test bench design in CAD. . . . .	35
4.2	From left to right: the target hole configuration, a hole displaying the “snowman effect”, and a barely allowable hole. The smaller blue hole represents the back-drilled pilot hole, and the larger red hole represents the final hole. . . .	37
4.3	This illustration displays the offset drill test. The drill bit was intentionally offset from the pilot hole, resulting in a curved back-drilled hole. The position of the original pilot hole $E_i$ and the final exit hole $E_f$ were both compared to a reference hole, and the difference was defined to be the position error. . . .	39
5.1	A cross section of the completed offset drill test. Note that the holes toward the right side of the image descend fairly straight through the surface, while as the holes approach the left, they become more and more slanted relative to the surface. This is due to the increasing drill offset from right to left. . . . .	42
5.2	This graph displays the position error observed relative to the offset error imposed, and the best fit line. . . . .	43
5.3	This graph displays the diameter deviations from the mean, measured in the $x$ and $y$ directions. . . . .	44
5.4	This graph displays the position error data. The $x$ - direction was defined as away from the drill, and the $y$ - direction was defined as to the left of the drill. Note that the average $x$ error is significantly more than the average $y$ error, and consistently positive. . . . .	45
6.1	These images display various options for the drill spindle configuration. (a) shows the configuration of the prototype that was tested for this thesis. (b) shows a new configuration where the suction cup still secures to the skin, but the drill spindle is now parallel to the spar. (c) shows a new configuration where the suction cup secures to the spar chord flange, while the drill spindle is parallel to the spar. . . . .	54
A.1	This graph displays the width of each bay. . . . .	67

A.2	This graph displays the length of each bay. This measurement represents the distance from the access hole in the center of the bay to the spar chord where back-drilling will be performed. . . . .	67
A.3	This graph displays the height difference between the last stringer and the spar chord in each bay. . . . .	68
A.4	This graph displays the horizontal distance from the last stringer and the spar chord in each bay. . . . .	68
A.5	This graph displays the height difference from the wing skin to the spar chord in each bay. Although the values range relative to each other, note that the absolute value is always less than an inch. . . . .	69
A.6	This graph displays the angle between the last stringer and the spar chord for each bay. As can be seen, some of these values are near 5 degrees, which is significant. Fortunately, unlike the five-axis platform, the manually operated pneumatic tool is mounted directly to the wing skin and avoids these large angles. . . . .	69
A.7	This Pugh Chart analyzed the long range positioning system. . . . .	70
A.8	This Pugh Chart analyzed the local positioning system, or arm design. . . . .	71
A.9	This Pugh Chart analyzed the various designs for an end-effector system. . . . .	72

## GLOSSARY

AFT: “after” or behind a given section of the airplane. From naval terminology.

BACK-DRILLING: a drilling procedure where a pilot hole is extended from the interior of the wing to the exterior, with the intention of guiding the position of the final hole from the opposite side.

FORE: “forward” or ahead of a given section of the airplane.

PILOT HOLE: an initial hole that is predrilled to provide a marked location for a later drilling procedure.

RIB: a vertical support structure within the wing between the upper and lower skin that runs parallel to the motion of the airplane. Ribs also act as the natural dividers between different wing bays.

SHEAR TIE: a flat tab that is designed to secure the wing skin to the edge of the rib.

SPAR CHORD: a long support structure at the leading and trailing edges of the wing, tying the upper and lower skin sections together.

STRINGER: a long, small, low profile support structure that runs along each skin of the wing, with a roughly Z-shaped cross-section. Designed to stiffen the wing skin.

WING BAY: an interior section of the wing that must be accessed for assembly work. It is bounded by a rib on each side, the upper and lower wing skins above and below, and the front and rear spar chords.

WING SKIN: the aerodynamic surface of the wing; smooth on the exterior and covered with stringers on the interior.

## ACKNOWLEDGMENTS

The author wishes to express sincere appreciation to the following parties, without whom this research project would not have been possible:

- The University of Washington, where he has had the opportunity to conduct this research and complete coursework.
- The Boeing Company, which generously provided funding and resources, and created this research opportunity.
- James Buttrick, who managed the project and provided guidance continually.
- Professors Joseph Garbini and Santosh Devasia, for their indispensable advice throughout the project.
- Terry Rowe, for his help with mechanical design and practical assembly.
- Alexi Erhlich, a fellow graduate student, who worked on different aspects of the same confined space automation project. A great deal of the documentation of spatial constraints and many design discussions were accomplished together.

## DEDICATION

To my parents, who have always encouraged me in my endeavors.

## Chapter 1

# INTRODUCTION

Commercial airplane manufacturing requires employees to crawl or reach inside individual bays within the wing to complete assembly work. This task is performed within a confined space testing the limits of human mobility with poor visibility, and hence frequently results in human error, injuries, and fatigue. This project was focused on developing a mechanical aid for back-drilling pilot holes in the interior of the wing. Back-drilling is the task of extending pilot holes from the interior of the wing through the wing surface to the exterior.

This research began with the premise of designing a mobile “crawler” robot, and eventually evolved into a human-guided semi-automated system. A five-axis drill platform was built, and preliminary testing revealed challenges of the design. This led to the final design of a smaller pneumatic tool that required more operator cooperation. In final testing, the pneumatic tool produced holes within the allowable tolerance, but more design iterations will be necessary before it can be implemented on the factory floor. This thesis describes the design process and test results of this manually operated prototype.

### ***1.1 Research Question***

Design, construct, and validate a mechanical system capable of fitting into the confined space of a commercial airplane wing bay, and drilling pilot holes to required tolerance.

Specific questions that this research was intended to address were:

- Is there a practical solution to augment an semi-automated drill system with current assembly procedures?
- What factors influence hole position and diameter errors, and what errors are allowable?

## **1.2 Thesis Statement**

During the manufacture of commercial airplanes, access to the internal structure becomes progressively more difficult as assembly is completed. This is especially true of wingbox assembly. Closeout of the wingbox is typically performed with the fastening of the lower wing panel. Mechanics must crawl or reach inside a small access hole and perform tasks by hand.

It has been proposed that a mechanized system could be designed to assist this process, thereby saving time and money during assembly. Specifically, this device would need to operate in the small confines of the interior of the wing, with as little human intervention as possible.

Back-drilling is a procedure that extends pilot holes from the interior of the wing to the exterior. Since these are pilot holes, and not a final procedure, they do not require inspection or certified tools. This makes back-drilling a simpler procedure than most other tasks, and therefore an attractive target for this first-generation prototype.

This proposal requires a small, lightweight, self-stabilizing drill system. This thesis will explore the design process that evolved during this research project, and describe the final test results and conclusions.

## Chapter 2

# BACKGROUND

This chapter describes the motivation behind this research project from a manufacturing perspective, and discusses the space constraints and proposed requirements of the design.

### **2.1 *Research Motivation***

This research was concerned with assisting in the assembly of commercial airplanes, such as the airliner pictured in figure 2.1. Automation research has become a priority to increase the rate of production and reduce repetitive stress to mechanics. The goal was to create a device that could work alongside mechanics to improve the speed and quality of the product, while improving comfort and safety for the employees.

Initially it was assumed that the device would need to be mobile, and work had already begun on a crawler as seen in figure 2.2. This crawler included folding tracked arms for maneuvering, but was eventually found to be too large for most wing bays.

### **2.2 *Assembly Environment***

This project focused specifically on wing assembly. The wings are assembled separately from the rest of the aircraft, and are composed of four main sections:

- Upper skin
- Lower skin
- Front spar chord
- Rear spar chord



Figure 2.1: A Boeing 737, which is in the general size range of the airplanes considered in this research. [1]

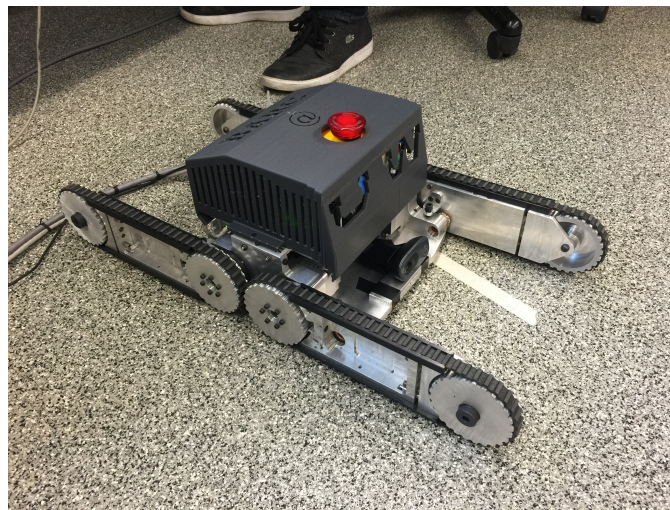


Figure 2.2: An early design of a tracked crawler with folding arms.

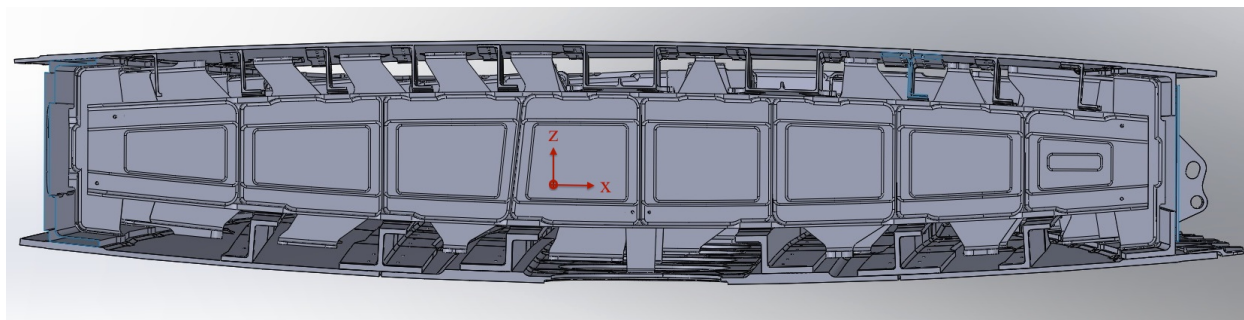


Figure 2.3: The cross section of a typical wing bay.

The cross section of a typical wing bay is pictured in figure 2.3. The order of assembly is such that the front and rear spar chords are first attached to the upper wing skin. This is fairly straight-forward, and does not require mechanics to enter confined spaces. The final procedure however, is much more complex. The lower skin is attached, and in order to apply the necessary fasteners to secure the skin, mechanics must climb or reach inside each wing bay section to perform assembly tasks. This is facilitated by the presence of an access hole in each wing-bay as pictured in figure 2.4, but remains an uncomfortable, slow, and difficult production task. The tight quarters often result in operator error and fatigue, which are both a liability.

The wing is divided into 26 different wing-bays, and each is unique due to the tapering nature of the wing. The wing bays vary substantially in size from the root to the tip of the wing. At the root of the wing, the bays are big enough for the mechanic to crawl inside, but require a great deal of mobility. At the tip of the wing, the bays are so small that the mechanic can barely fit more than their forearm and the required machine tool.

The goal of this project was to design a system capable of working alongside the manual operator to improve the speed and quality of these tasks. Ideally, the manual operator could stand outside the wing, and direct the motions of the system without entering the wing. To test the approach, back-drilling pilot holes inside the wing was the first task that was chosen.

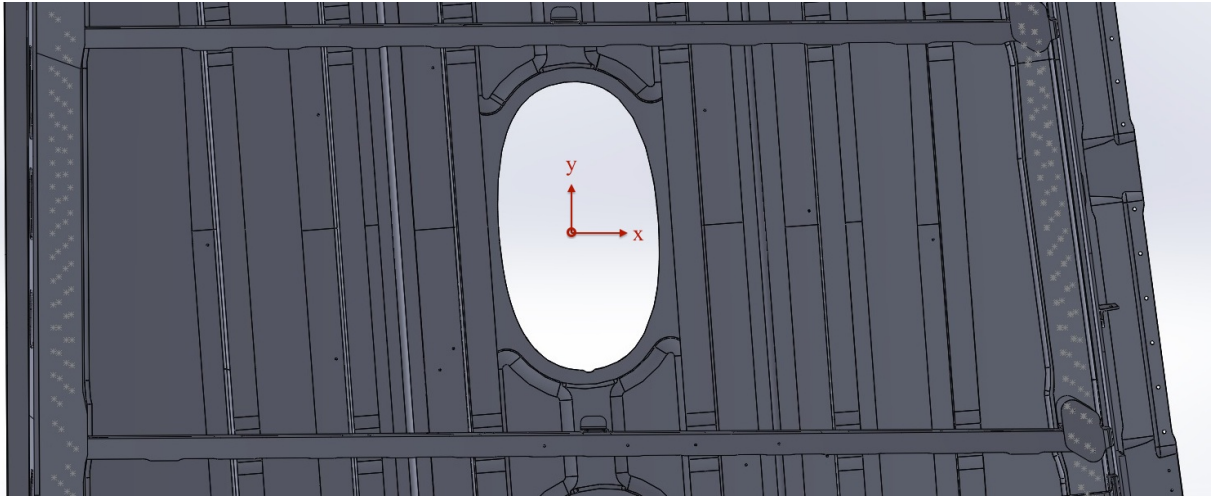


Figure 2.4: The view of a typical wing bay as seen from above. Note the access hole and the placements of marks signifying hole locations on the spar chord flanges at each end.

### **2.3 Back-Drilling**

Due to the desire to create a functioning and practical prototype in a reasonable timeframe, the task of back-drilling pilot holes was chosen as the target procedure. There are other tasks performed in the wing-bay space, but they are all more complicated. Back-drilling was considered a reasonable task to demonstrate the feasibility of this first prototype iteration.

During wing assembly, the front and rear spar chords each feature a flange with pilot holes, as seen in figure 2.4. Once the lower wing skin is attached, these pilot holes must be extended through the wing skin. This pilot hole extension is the back-drilling procedure, and must be performed from inside the wing. This new pilot hole is used to locate the final, larger hole from outside the wing as seen in figure 2.5.

One of the biggest obstacles in automation research for aerospace manufacturing is the strict requirements that only tools that are certified for a particular operation are used. These tools have been tested and found adequate for the specified tasks, and therefore a non-certified tool cannot be substituted.

Unfortunately, this requirement is restrictive to the research of automation equipment,

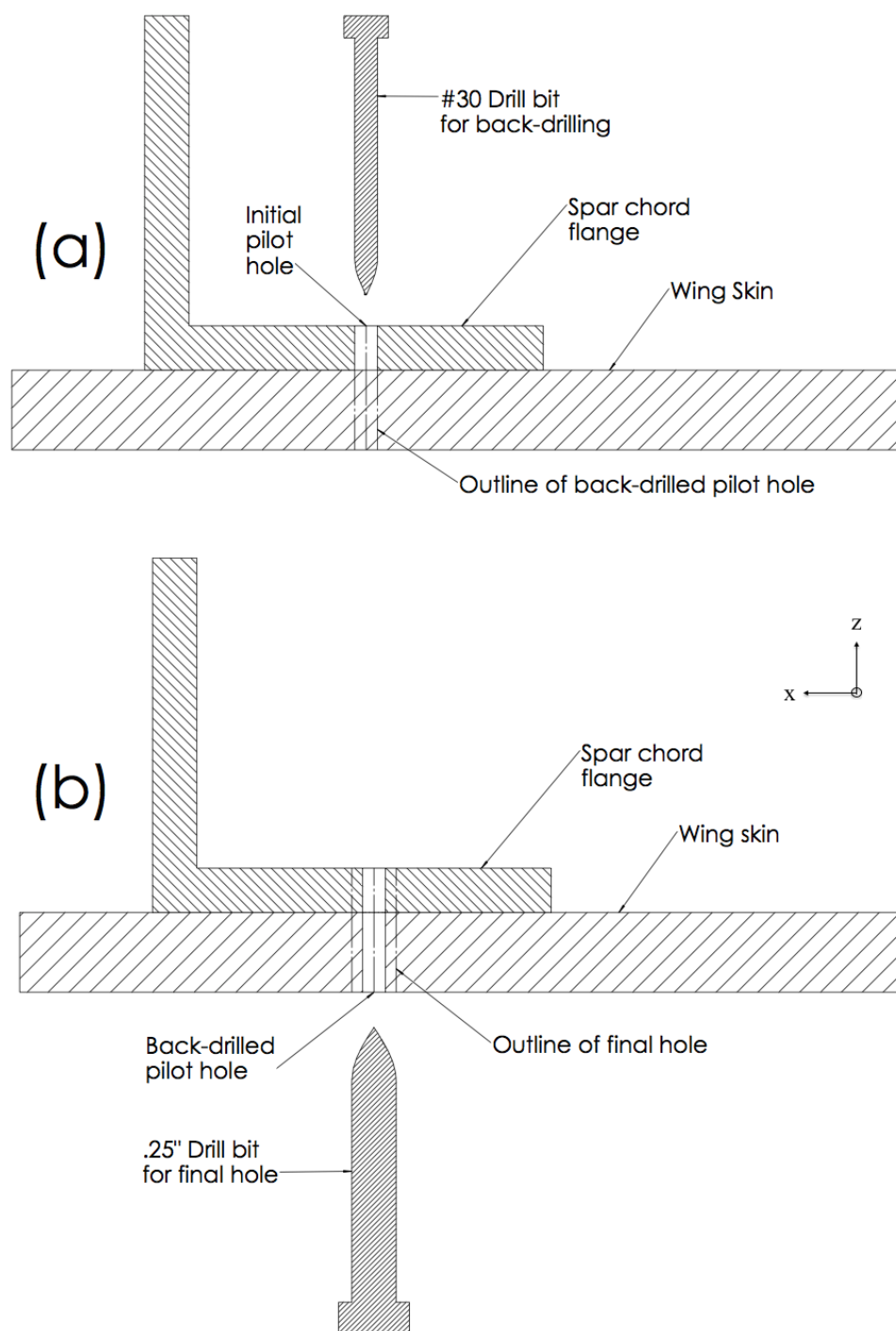


Figure 2.5: This figure illustrates the back-drilling procedure. The purpose is to extend an initial pilot hole on the interior of the wing to the exterior of the wing, as shown in (a). This exterior pilot hole will provide the location for the final drill procedure, which will be completed with a larger drill bit from the outside of the wing as shown in (b).

since the certification process is arduous, and the currently certified tools are designed for manual operator use. Typically, a different tool or a modified manual tool would be more effective and space-efficient for an automation system, but such tools are not certified. Additionally, aerospace manufacturing requires inspection for features on the completed airplane.

This makes the back-drilling process a promising initial goal for the first generation of this confined-space mechanical system. The back-drilling procedure is *not* the final hole, and is merely a pilot hole. Later, the inner surface of the pilot hole is removed by the drilling of the final, larger hole. Since these back-drilled pilot holes are *not* ending up on the final airplane, they do not require certified tools, and do not need to be inspected. This allows the first generation of this confined-space device to experiment with changes in optimal tool design.

## 2.4 Literature Review

Automation is a frequently researched topic in mechanical engineering design, and as a result there is a great wealth of published work on the topic. However, each application is specific enough that most existing literature provides only minimal instruction of a cursory nature.

Some research papers dealt specifically with the problem of long-range maneuvering for the system. The paper *Analysis, Design, and Control of an Omnidirectional Mobile Robot in Rough Terrain* [2] explored the utilization of a “split offset caster drive mechanism” to allow the robot to move in any direction over uneven surfaces. The drive mechanism employed wheels on casters that could rotate, mounted on a suspension system that allowed for vertical motion as well. It is the kind of system that is tailor-made for a Mars explorer, but likely impractical for confined space airplane assembly. As will be discussed later on, the vertical nature of the stringers within the confines of the wing bay prevent wheels from being a likely solution.<sup>1</sup> However, the analysis of such papers proved to be useful background research.

Several papers dealt with the design and control of robotic end-effectors to perform

---

<sup>1</sup>See section 3.3.1.

specific tasks in a given domain. The papers *Kinematic Design of a 5-DOF Hybrid Robot with Large Workspace/Limb-Stroke Ratio* [3] and *A Mechatronic Design Process for Three Axis Serial Robots* [4] both dealt with work in specified domains, but they did not have confined space limitations and therefore were allowed plenty of room for joint retraction and limb motion.

Another paper, *On the Design of a Mechanically Programmable Underactuated Anthropomorphic Prosthetic Gripper* [5], dealt specifically with making a compliant end-effector system. This was of interest because the natural compliance of the human hand is what allows manual operators to achieve accurate back-drilled holes, despite limited visibility in the wing bay. Mechanics simply feel for the pilot hole, begin drilling, and the results are satisfactory. During much of the design process it was assumed that some sort of compliance would be necessary to ensure that the mechanical drilling system would accurately drill through the pilot hole, and this paper provided a guideline for how such a design might proceed. As will be discussed further on, such a compliant system was deemed unnecessary and was never pursued to any great length.<sup>2</sup>

Additionally, there were multiple papers that combined the above design problems, and endeavored to establish a design that dealt with long range positioning as well as the localized end-effector for specific tasks. The papers *Mobile Robotic Assembly on a Moving Vehicle* [7] and *Mechanical Design of a Robotic System for Automatic Installation of Magnetic Markers on the Roadway* [8] both dealt with practical applications for moving robots that would need to perform assembly work. Again, these devices did not have the same space constraints or local obstacles that are present in the wing bay, but provided useful reference for such design work.

The paper *Design and Analysis of a Hybrid Mobile Robot Mechanism With Compounded Locomotion and Manipulation Capability* [6] was the most relevant and inspiring. It featured a small robot intended for confined space applications that utilized rubber tracks for

---

<sup>2</sup>See section 3.3.4.

manuvering and a collapsible articulated arm for performing work. Early on in the design process it was still assumed that a mobile system would be the eventual goal, and the robot described by this paper most nearly fit the ideal that was being worked towards. As will be described in chapters three and four, a mobile system was eventually tabled for a future project. Additionally, while the arm for this system was ingenious in its ability to retract and virtually disappear from view, it still required more vertical space to maneuver than would be allowed for in the wing bay.

## Chapter 3

# DESIGN PROCESS

This chapter describes the entire design process, evolution, and rationale behind the mechanical system considered in this thesis. Since this thesis is intended to be useful as a process guide for similar mechanical design projects in the future, attention will be given to abandoned design concepts.

### ***3.1 Design Approach***

The design process began with an emphasis on practicality, but without initially discouraging radical design proposals. All forms of design concepts were encouraged and thoughtfully considered. The intention was to start broad, consider many solutions, and narrow down the concepts based primarily on practicality.

In order for the project to be a success, the final design would need to display promising results from a practical point of view. This required that the design be easily compatible with the current manufacturing process, and not disruptive or time consuming to use. It required a system that needed minimal support, and not require any fundamental changes

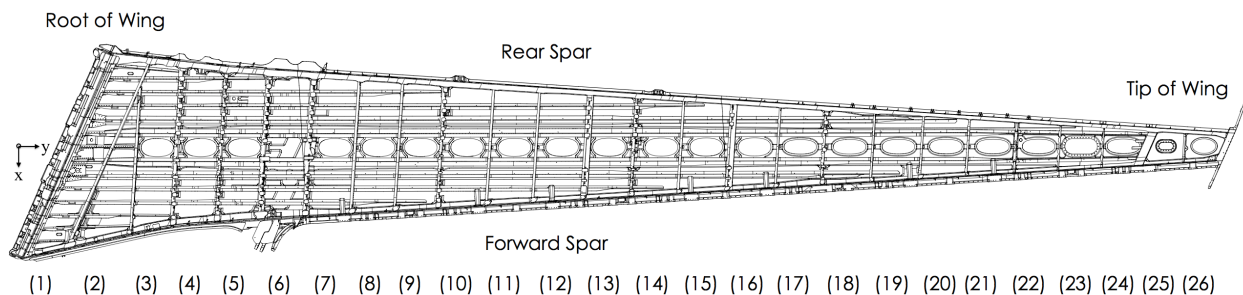


Figure 3.1: The wing model as seen from above, with the wing bays labeled by number.

to the assembly environment. Of course, it needed to be reliable and robust.

It was recognized that the concept that was eventually chosen and manufactured would still not be a truly *final* design. It would merely be the first iteration of a series of designs that would lead up to a practical solution that could be produced in large quantities and implemented on the factory floor.

One of the philosophies adopted in this design approach was referred to as the “80 percent solution.” Since each bay of the airplane wing vary somewhat in shape and dimensions and some have unusual obstacles present, it was decided early on that developing an automation system that could complete *most* of the work would be sufficient. Attempting to design a system capable of performing 100 percent of the work would likely be unfeasible for this first design iteration.

By choosing to focus on an “80 percent solution”, the early prototypes could be completed much more quickly. This permitted testing to be completed earlier, which allows designers to “learn by doing”. With the knowledge of early test results, future designs will prove more practical and evolve more quickly.

### **3.2 Design Constraints**

The first task was to characterize the system operational space. A 3D model of a commercial airplane wing was analyzed to facilitate in this documentation phase of the project. Each bay was measured dimensionally and evaluated qualitatively on obstructions and other irregularities present. Several graphs were created from the wing bay data, such as the graph of bay height in figure 3.3.

Each wing bay is unique, which presents a serious challenge to creating a single mechanical system that could perform tasks within the entire wing. Some of these differences can be observed in figure 3.2, which includes four different wing bays with notable features labeled. At the base of the wing, each bay has plenty of headspace, but is lengthy, and would require some kind of mobile system capable of traveling down the length of the bay. Toward the middle of the wing, each bay becomes progressively lower in height, dramatically reducing

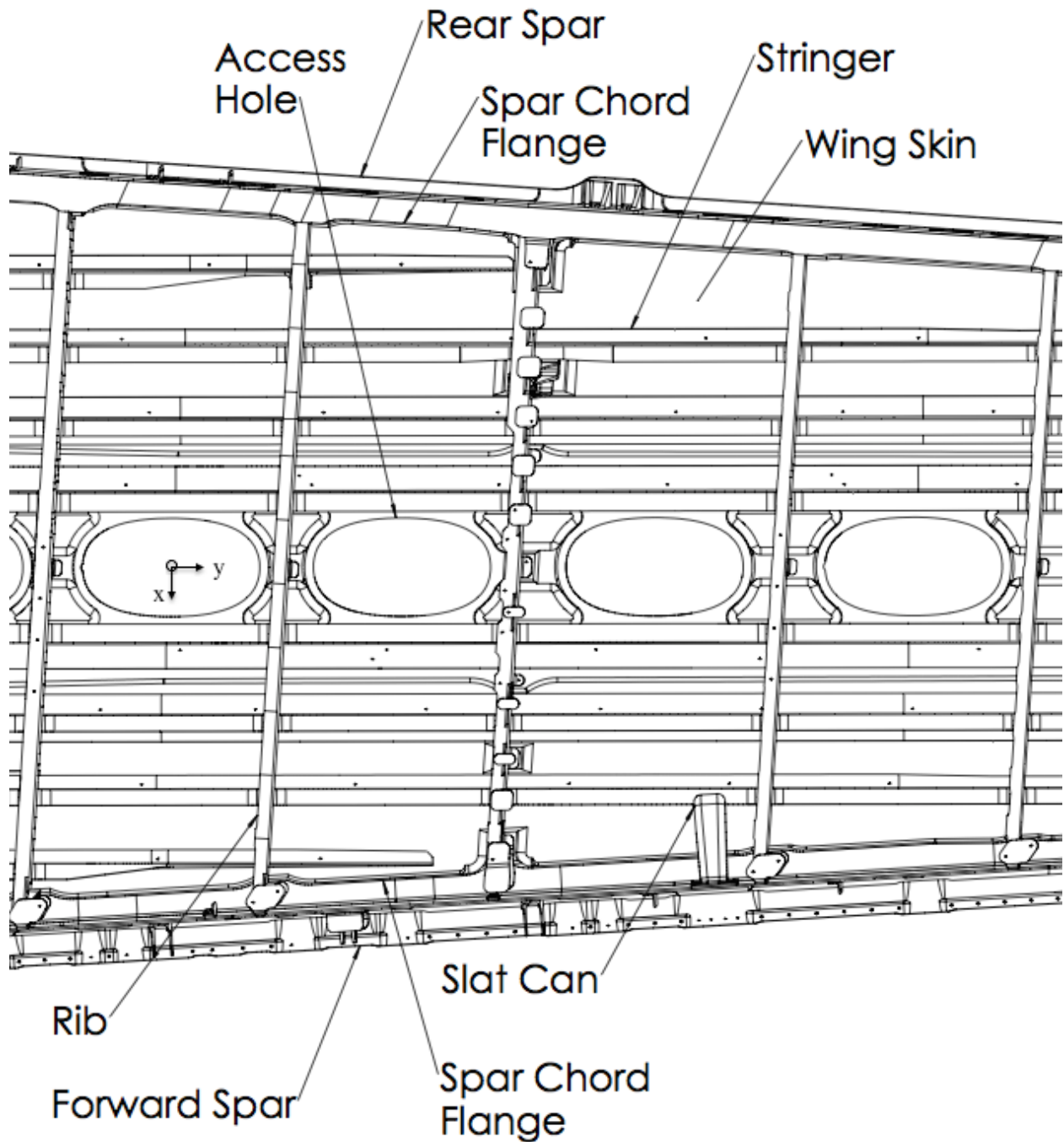


Figure 3.2: A closer image of the wing bays from above. Several notable features are labeled, such as the access hole and spar chord flanges.

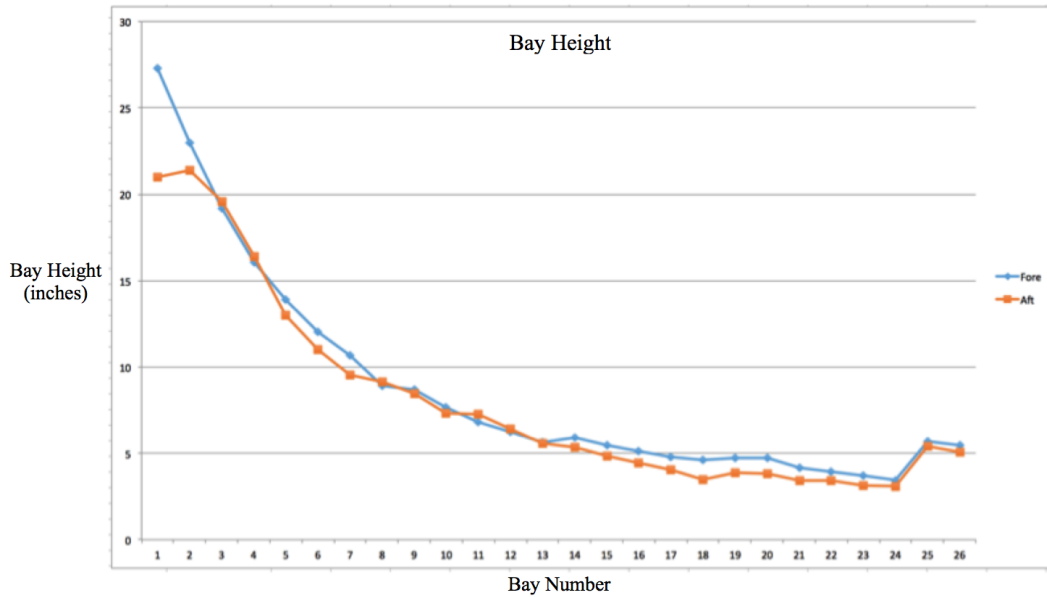


Figure 3.3: This graph illustrates that the wing bay height rapidly decreases as the end of the wing is approached. See the appendix for similar graphs.

the space for the operator or the device to maneuver. As the end of the wing is approached, each bay becomes impossible for an operator to enter, and can only be accessed by hand. However, these outer bays are short enough in length to eliminate the need for a mobile system, and a stationary system would likely be sufficient.

While some of the bays have unique challenges, some aspects are shared by all. Each bay has a “rib” along each side, serving as a support structure and a divider between the next bay. At each end of each bay there is the front and rear spars, which is where the majority of the back-drilling procedure is performed. Along the upper and lower wing skins, there are “stringers” that run from the inboard end of the wing until they terminate further along the length of the wing. There are many stringers at the root of the wing, since the wing is wide at that point. As the tip of the wing is approached, there are fewer stringers because the wing is much narrower. That transition is made by stringers “running out” (or ending) as the edge of the wing approaches them. These stringers create an uneven and irregular surface for the operation of the system.

Some of the bays have unique considerations. Three of the bays lack an access hole, and must be accessed from an adjacent bay by crawling through a hole in the rib. Several of the bays have a large obstruction protruding from the web of the spar chord that is referred to as a “slat can”.

Even more critical than the wing bay dimensions are the dimensions of the access hole. If the device cannot fit through the access hole, then it cannot perform tasks within the wing.

Physical space limitations were not the only design constraints. The system would also need to be at least as fast or faster than the current process for back-drilling. Even if this system ends up being more expensive initially, it would have a good chance of being implemented if it could prove faster at drilling holes than the current method.

Other constraints imposed were based on the design goals; the system should be as simple as possible, safe, easy to operate, and lightweight to facilitate manual placement. These constraints were quantified by using the existing manual drilling procedure as the standard for comparison. The goal was to create a system that met or exceeded the abilities of the manually operated drill. It would ideally be safer and easier to operate than the current method, and would be lightweight enough to allow an operator to manually insert it into the wing. This weight was determined to be 30 lbs at maximum, with a goal of 10 lbs.

### ***3.3 Preliminary Design Process***

Once the design constraints were well analyzed and understood, the time came for proposing design concepts. To simplify and organize the conception of new design concepts, the system was broken into several key subsystems. Each of these different components would have a variety of design proposals considered and compared.

After some refinement, candidate designs for each subsystem were incorporated into a Pugh Chart for comparative analysis. One design concept was chosen as the “baseline”, and the other design concepts were compared to it. Then a list of requirements are created, and for each requirement, each design is rated as better, worse, or equal to the baseline. The results are totaled at the bottom of the chart, and it is easy to observe which designs are

superior or inferior to the baseline. One drawback of the Pugh Chart however, is that it is not a weighted design matrix. This means that all requirements are weighted equally, which is rarely the case in reality. Therefore, it is important to consider that a Pugh Chart is useful for comparison and reference, but the most practical design for a given application may not be the concept with the highest accumulated score. A different Pugh Chart was used for each subsystem considered.

The subsystems considered were:

1. Long range positioning system
2. Local positioning system
3. Stabilization system
4. Compliant drilling system

The following sections describe each of these subsystems, the proposed designs, the chosen design, and the rationale behind the final decision. The Pugh Chart for the stabilization system is shown in figure 3.4, and the other Pugh Charts can be found in the appendix.

### *3.3.1 Long Range Positioning System*

From the beginning of this research project it was assumed that the automation device would be a crawler of some sort. A mobile robot was envisioned that would maneuver from the access hole in the center of the bay to the spar chord at the end of the bay where most of the drilling takes place. Hence, one of the main design considerations was what sort of positioning system would be utilized to maneuver the robot from one location to another. This component was referred to as the “long range positioning system” to differentiate it from the “short range positioning system” which is described in the following subsection.

There are several different methods for maneuvering vehicles. Cars have wheels, tanks and most construction equipment have tracks, trains have rails, some robots have legs, and there

are even cable robots that span a domain with cables. All of these ideas were entertained and compared on the Pugh Chart for a variety of requirements.

Rails were agreed to be the most stable. Most mill systems operate entirely on rails. However, installing them within the confined space of the wing bay presented a challenge. Because the purpose of this research was to reduce the amount of work and effort for the wing assembly mechanics, adding another task within the wing ran contrary to the goal of the research.

Rubber tracks were recognized to be less stable than rails, but much simpler to operate and more versatile. A tracked system could be inserted into the wing bay and crawl across the stringers to the spar chord at the end.

Wheels and legs were recognized as impractical due to the presence of the stringers, and a cable robot was ruled out due to the lack of available height.

It was eventually recognized that height constraints were going to become the driving factor behind the design. Only the first few bays of the wing are tall enough to fit a crawler system carrying an end-effector. Moving away from the fuselage, the wing quickly tapers to a lower height.

Fortunately, as it tapers to a lower height, the distance from the access hole to the spar chord is reduced. This allows the spar chord to be accessed by hand without requiring a mechanic to climb inside the bay. This makes it feasible to design a stationary platform system that can be inserted into the wing manually.

### *3.3.2 Local Positioning System*

Regardless of how the device arrives at the end of the bay, it will need some form of mechanism to position the tool and complete the task of drilling holes in the spar chord. This was referred to as the “local positioning system”.

One concept was an  $x$ - $y$  horizontal traversal system mounted on a rotating link, with a vertical  $z$ -axis at the end of a cantilever to mount the tool. This was referred to as the “tank turret” concept, due to the rotating link at the base. This system was chosen as the

baseline.

A centralized, more traditional looking robotic arm with at least three serial links was proposed as another design. It would have been more flexible and easier to insert into the access hole, but would have been more difficult to maneuver due to height constraints.

One proposed concept was a curved rail around the perimeter of the device, with a small, localized arm that could use this rail for local moves. This system was seen as space efficient and sturdy, but presented a challenge to easily manufacture, and would be difficult to fit through the access hole.

Several other concepts were considered, including a conveyor belt, a turntable platform, and a mobile rail system, but all were deemed too complex for this application.

Eventually, a five-axis arm design was chosen that combined traits from several of the original concepts. It had low profile rails for the horizontal  $x$  and  $y$  axes, vertical rails for the  $z$ -axis, and two rotation axes for ease of maneuverability and to ensure all pilot holes could be reached by the drill system.

### *3.3.3 Stabilization System*

In order to properly drill a hole, the device would need some form of stabilization mechanism to provide reaction force for the drilling procedure and ensure that the system would not move or shift while drilling.

The first aspect in stabilization that must be identified is what features in the local environment are suitable to use for stabilization. The interior of the airplane wing is sturdy, and offers a variety of surfaces that can be used to anchor the system.

Most obviously, there are the stringers. The stringers are fairly uniform in shape and alignment, and provide one of the most predictable features in every wing bay. However, it is worth noting that the stringers are not parallel to the spar chord where the work will be performed. Due to the tapering of the wing as it narrows toward the end, the stringers in every bay are a different distance away from the spar chord. So while the shape of the stringers is consistent, their position relative to the spar chord is not.

	Group	Requirement	Baseline	Concept 2	Concept 3	Concept 4	Concept 5
Stabilization System			Clamping to stringers	Suction cups to skin	Compliant Pressure Foot	Backhoe legs	Magnet coupling
	Spatial	Fits through hole		S	-	S	S
	Spatial	Height fits wing tip		S	-	-	S
	Time	Local 10 seconds		S	-	S	S
	Stability	Stable end effector to .01"		S	-	-	S
	Stability	No moment on stringers		S	S	S	S
	Operation	Cost		-	-	S	-
	Operation	Size of umbilicle		S	-	S	S
	Operation	Energy intensity		-	-	S	-
	Operation	Ease of use		+	+	+	-
	Manufacturing	Easy to manufacture		S	-	S	-
	Manufacturing	Design Cost		+	-	S	-
	Manufacturing	Time		S	S	S	S
	Manufacturing	Complexity		+	-	+	S
			+	3	1	2	0
			-	2	10	2	5
			S	8	2	9	8
			total	13	13	13	13
			score	1	-9	0	-5

Figure 3.4: This is the Pugh Chart that was analyzed for the stabilization system. See the appendix for similar charts of other systems.

Another fairly uniform surface to consider is the lower wing skin. However, the diverse positioning of the stringers again creates complications. The available skin area between the last stringer and the spar chord in each bay is not uniform.

The baseline chosen for the stabilization system was clamping to the stringers. This initially appeared to be the most obvious stabilization solution, and would certainly offer a significant amount of rigid stability. However, the horizontal profile of the stringers posed a challenge when actually attempting to create a practical clamp design. Since the device would need to fit through the axis hole and slide across the stringers, the clamps would initially need to be rotated out of the way, but would eventually need to rotate into place and clamp to the stringers. The number of actuators to sufficiently clamp such a system was deemed unnecessarily complex.

The second concept was the utilization of suction cups to attach directly to the wing skin surface. This would not necessarily require any actuators at all. However, it would be slightly more compliant and less rigid than clamps to the stringers.

Other concepts included adjustable feet referred to as “backhoe legs” that would press against the wing surface, a “compliant pressure foot” that could change shape to match a feature and then expand or contract to secure itself, and a magnet coupling system that would require magnets on the device as well as outside the wing. The Pugh Chart in figure 3.4 shows how these concepts compared on meeting various requirements.

Ultimately, the suction cup concept was chosen as the most reasonable design. It would be stable, have more options on placement, would be cheap and easy to use, and fairly simple.

### *3.3.4 Compliant Drilling System*

Throughout much of the design process, it was assumed that the system would require compliance in the  $x$ - $y$  directions to accurately place the drill within the pilot hole. The manual method for back-drilling holes employs the use of a human hand, which uses compliance to accurately locate and drill through the pilot hole within the wing, with little to no visual aids.

It was assumed that compliance would be needed for two purposes: first, to ensure that the drill position matched the position of the pilot hole, and second, to ensure that the back-drilling procedure was performed orthogonal<sup>1</sup> to the spar chord surface. Several preliminary concepts were pursued and discussed with these two objectives in mind.

Eventually, it was decided that compliance would be unnecessary for this first generation prototype, and would add significant complexity to the system. However, future designs would likely need to incorporate compliance.

For positioning inline with the pilot hole, it was decided that the allowable error would need to be determined, and tests would be performed to evaluate whether the system would be capable of meeting such error requirements. The test that was designed is referred to elsewhere in this thesis as the “offset drill test”, and discussed at length in chapters four, five, and six.

For orthogonality with respect to the drilled surface, it was decided that the typical angle difference between the wing skin and the spar chord would need to be determined before compliance was pursued. Based on the analysis of the wing bay, the spar chord is never more than 1.5 degrees off from the wing skin locally. This was determined to be small enough for creating adequate back-drilled holes.

### **3.4 Five-Axis Stationary Platform**

Based on the above process of preliminary design work, a concept was settled on for a five-axis stationary platform. This device was a flat, low-profile system that could be inserted through the access hole, and easily slid across the stringers by the mechanic, without requiring an operator to actually enter the wing with their body. Figure 3.5 demonstrates an early model of the design virtually fitting in the wing bay.

This system was equipped with suction cups that would engage the top surface of the stringers, and a five axis arm system that would operate the drill. The  $x$  and  $y$  axes were

---

<sup>1</sup>Orthogonal is an engineering term that means perpendicular, but specifically perpendicular to an entire plane, not just a single line.

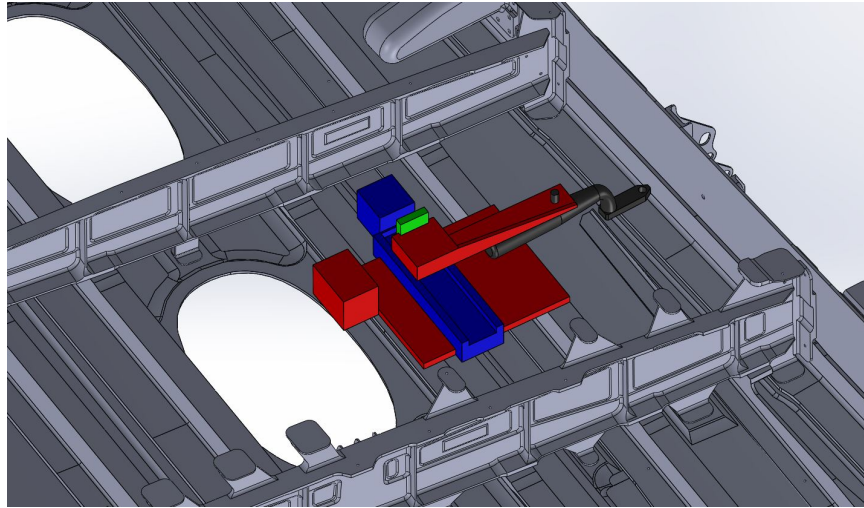


Figure 3.5: An early design mockup of how the platform system might fit within a typical wing bay.

each powered by electric motors with encoders to ensure accurate control and positioning. These motors utilized a rack and pinion drive mechanism to drive the system along linear guide rails. Figure 3.6 shows the final model of the design.

The five-axis platform system was tested on the test bench<sup>2</sup> to observe whether it could reach the intended domain, could properly secure itself by employing suction cups on the stringers, and could drill satisfactory holes. The physical prototype of the five-axis platform is pictured mounted on the test bench in figure 3.7.

It was observed after preliminary tests that the suction cup system was sufficient and the device could reach a satisfactory portion of the domain. However, the  $z$ -axis had trouble rising vertically, and the task of drilling would create an undue amount of bending in the cantilever arm.

The  $z$ -axis was powered by an air cylinder for simplicity, and originally traveled on cylindrical rails. But after disappointing results in preliminary testing, where the  $z$ -axis was unable to rise without aid, the cylindrical rails were replaced by precision linear guide

---

<sup>2</sup>See section 4.1 for more information on the test bench.



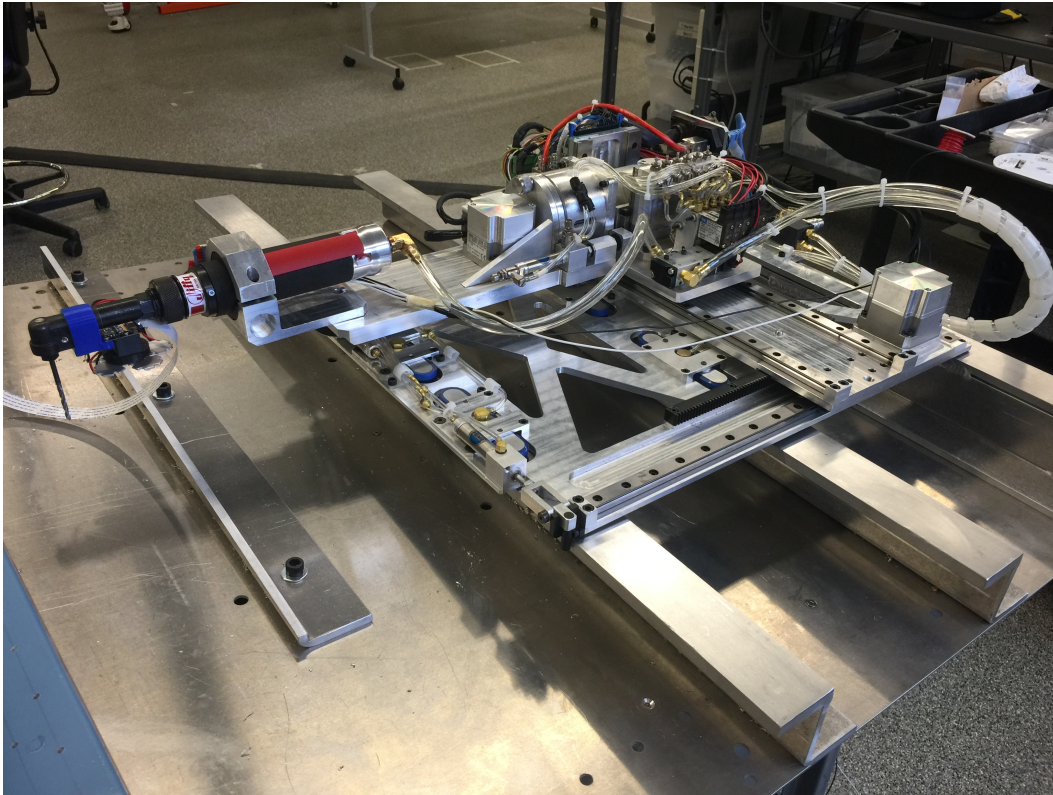


Figure 3.7: The final design of the platform system.

take place while drilling, and resulted in elliptical holes. The air-powered rotary axis about the  $x$ -axis was completed redesigned with a heavy bearing system to stiffen the cantilever. While this change proved to be an improvement, future preliminary tests found it to be insufficient as discussed below.

All possible efforts were made to reduce the height and overall size of this system. However, there were constraints that continued to increase the dimensions of the design. One of these constraints was the varying distance from the stringers to the spar chord. This forced an increase in the overall length of the arm and travel of the arm in the  $x$ -direction, since the spar chord would be quite close in some locations, and much further in others.

### *3.4.1 Challenges with the Design*

Several challenges were encountered with the construction and preliminary testing of the five-axis platform.

The first challenge was the most egregious; the system was simply too large. This platform would fit into some of the wing bays, but only about the first third of them, toward the base of the wing. This is because while the system is short enough to fit in more than a third of the bays, it cannot make it through the access holes on most of them without hitting the stringers on the upper wing skin, which is the ceiling of the bay.

The second challenge was that the cantilever of the arm allowed too much bending to take place. This bent the drill and created elliptical holes.

Concept designs have already begun on a new five-axis stationary platform system, taking the aforementioned problems into consideration. The next generation of the system will be designed to be lower profile, and have a more sturdy arm configuration.

However, even with the proposed design improvements, the stationary platform would never be able to reach all of the wing bays. Clearly, a new design was needed, ideally a smaller system that had a more local stabilization mechanism for offsetting the drill force.

## **3.5 Manually Operated Pneumatic Tool**

It was recognized that for the small bays toward the end of the wing, what was really needed was a simple system that could aid the operator directly. This system became the manually operated pneumatic tool, as pictured in figure 3.8 and 3.9. It was designed with a lengthy handle to prevent the need of the operator to reach too far inside the wing bay.

The five-axis platform system grew too large because it was designed to reach all of the pilot holes along the entire spar chord without being moved. For this new design, that goal was abandoned entirely. What was needed was a very simple system that could potentially have a faster rate of design and production, and enter the assembly floor as soon as possible. To do this, the system would have to work together with the current mechanics. Rather than

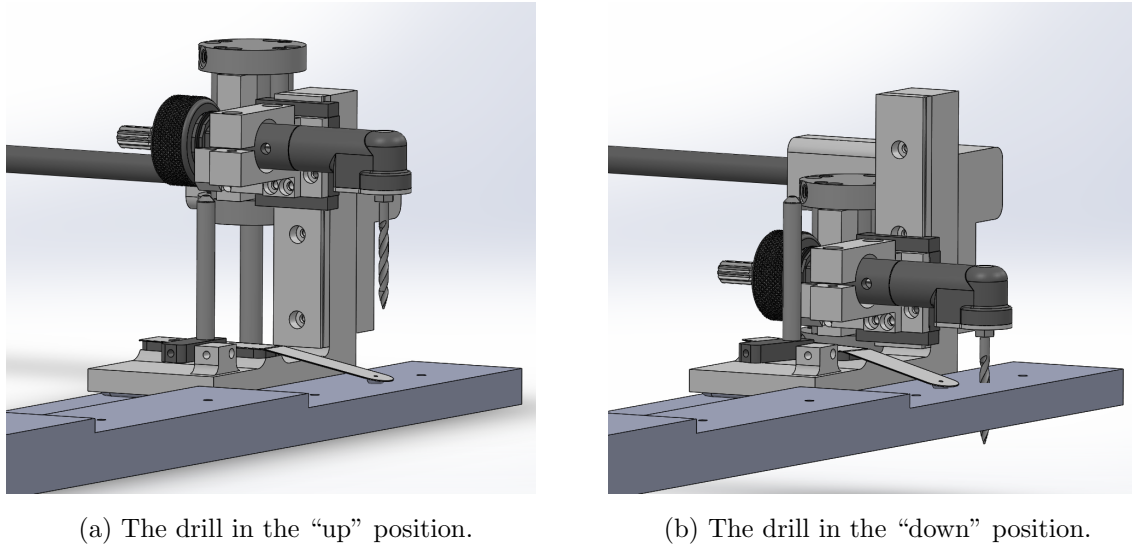


Figure 3.8: The above figures display the CAD design in Solidworks of the manually operated pneumatic tool. Note that the “locator pin” swings out of the path of the drill bit during drilling.

removing them from the bay entirely and having them drive the device from a distance, this new system would require them to manually move it from pilot hole to pilot hole. This was deemed reasonable and still an improvement, because it eliminates the need for mechanics to reach far into the wing bay or climb inside.

To avoid the challenges of the cantilever in the previous design, this system would need to stabilize as near to the actual drill operation as possible. The proposed solution was to suction to the wing skin immediately between the spar chord and the last stringer in the bay. This would ensure a small moment arm if any torque was created by the drilling operation.

The system was driven pneumatically for safety, simplicity, and weight savings. The vertical upward and downward axis for the the drill spindle was driven by an air cylinder. It was considered that an air cylinder would be sufficient since there were only two necessary positions for the drill; up for positioning, and down for drilling. The air cylinder would provide a constant downward drill force during the back-drilling procedure. The drill spindle

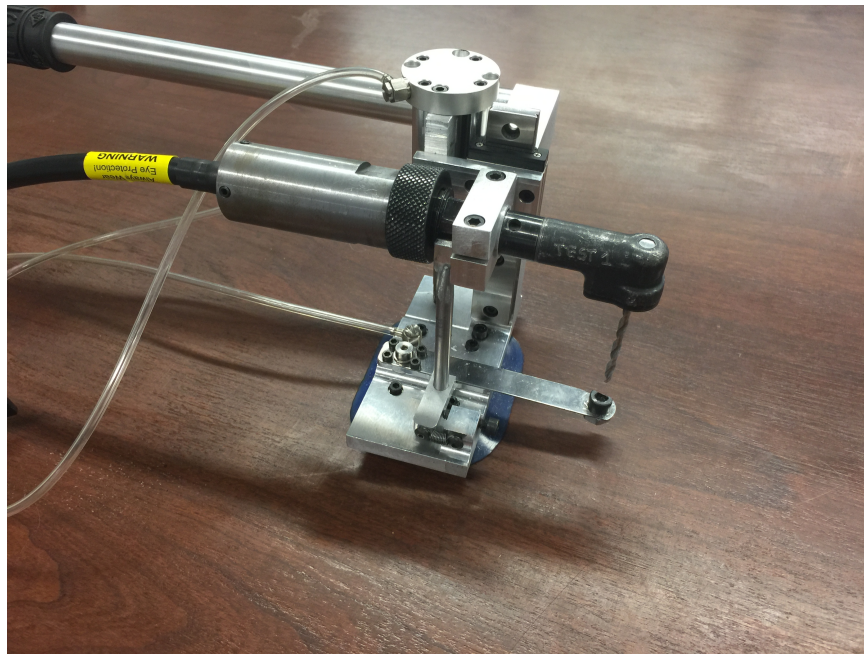


Figure 3.9: The completed prototype for the manually operated pneumatic tool.

itself was powered by an air motor with the utilization of a flexible drive shaft, and the suction cup was powered by a vacuum.

### 3.5.1 Suction Pad

Again, a suction cup was seen as the best way to secure and stabilize the system, and provide reaction force for drilling. Initially the suction cup was custom-made using a firm o-ring with a square cross-section. This custom o-ring suction cup design was intended to be more rigid than a traditional suction cup, lending stability to the system. However, early test results for the custom o-ring suction cup were disappointing. The suction cup would frequently pop off the surface during testing, since it was too rigid to withstand any significant bending of the system during drilling. The system would only retain a sufficient vacuum on a pristine surface. If there were any debris present or a scratch in the surface, the suction pad would not hold vacuum and would pop off the surface.

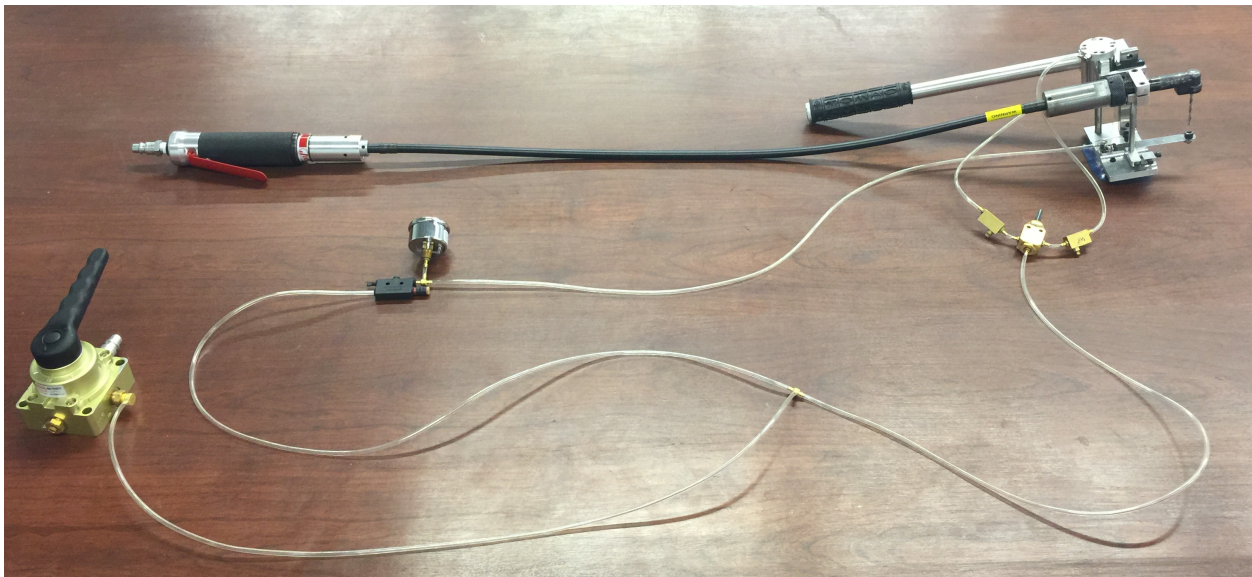


Figure 3.10: The manually operated pneumatic tool including the air motor, flexible drive shaft, and air supply system.

Due to these early test results, the custom o-ring suction cup was replaced with a commercial suction cup. This suction cup was much more durable, and would hold a sufficient vacuum regardless of the presence of debris or scratches in the surface. It had a smooth lip seal that allowed it to glide smoothly across surfaces, which facilitated in positioning. Due to the more compliant nature of this new suction pad, the system would not lose vacuum when the device would bend during drilling, but would also do little to prevent this bending.

To prevent excessive bending of the system during drilling, and ensure that the hole was close to orthogonal to the surface, the device needed a way to offset the moment from the drill force. This was accomplished by placing a wedge between the handle and a stringer. Figure 3.13 shows the pneumatic tool inside the wing bay for reference.

These preliminary tests also revealed that the rubber edged clamp that secured the drill spindle to the device allowed for too much compliance. It was replaced with an entirely metal clamping system, and much less bending and motion was observed during drill operations.

### 3.5.2 *Locator Pin*

One significant difference between this manually operated pneumatic tool and the five-axis platform was how it locates each pilot hole. With the platform, a vision system had been coordinated to allow the control system to recognize the outline of a hole, and position the drill bit over it. However, this is impossible for manual operation. Manual operators do not find holes visually alone, but also by touch, feeling for tactile feedback.

With that in mind, a round pin was designed that could glide across the surface of the spar chord flange and drop into any hole it encounters. This pin was positioned on the end of a flexible metal cantilever that acts like a stiff spring. The spring-like nature of the cantilever arm ensured that the pin would drop into holes when it encountered them, and ensured that the operator could receive tactile feedback to tell whether a hole had been located or not.

This pin was designed to remain inline with the drill for positioning, and slide out of the way during the drilling operation. It was referred to as the “locator pin”.

This procedure can be observed by comparing figure 3.8 (a) and (b). Initially, the locator pin is directly below the drill bit, and is used to locate a pilot hole. Once the suction pad is engaged, the drill is turned on and begins to descend toward the wing surface. A sliding mechanism causes the cantilever arm to swing out of the way as the drill spindle lowers. By the time the drill bit has reached the surface, the locator pin is successfully removed from the drill path. Once the back-drilling procedure is complete and the drill returns to the upright position, a spring will swing the cantilever arm and locator pin back into place. The locator pin on the cantilever arm can also be seen in figures 3.9, 3.10, and 3.13.

### 3.5.3 *Flexible Drive Shaft*

A common challenge for both the five-axis platform and the manually operated pneumatic tool was the weight of the drill motor. It is a substantial air motor, and for the pneumatic tool it would make up nearly a majority of the total weight.

Fortunately, as outlined earlier, back-drilling is not a final operation. Therefore, certified

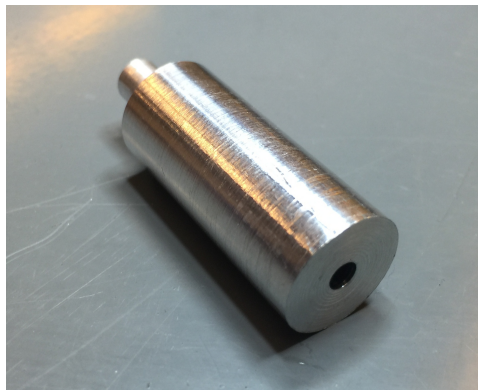


Figure 3.11: The alignment device.

tools are not required, and modified tool systems are permitted.

It was proposed that a flexible drive shaft could allow the heavy drill motor to remain outside the wing, while the smaller drill spindle performed drilling operations.

Several commercial flexible drive shafts were ordered, and a custom aluminum coupling device was designed for each end to interface with the drill spindle and the air motor as seen in figure 3.10.

This innovation dramatically reduced the weight and dimensions of the pneumatic tool, allowing it to fit into more bays and reducing strain on the operator.

#### *3.5.4 Alignment Device*

It was recognized that the locator pin innovation would be inaccurate without some form of alignment device to ensure that the drill was positioned in-line with the locator pin. This device would need to ensure the positioning of the drill spindle in the  $x$ -direction as well as the rotation of the drill spindle grip, and also to align the rotary position of the locator pin.

The alignment device that was built was a small cylinder with a hole in the top, and a smaller cylinder protruding from the base as seen in figure 3.11. The smaller cylinder would be inserted into the locator arm, and the drill bit would be inserted into the hole at the top as seen in figure 3.12. This would allow the drill to be easily aligned at any time.

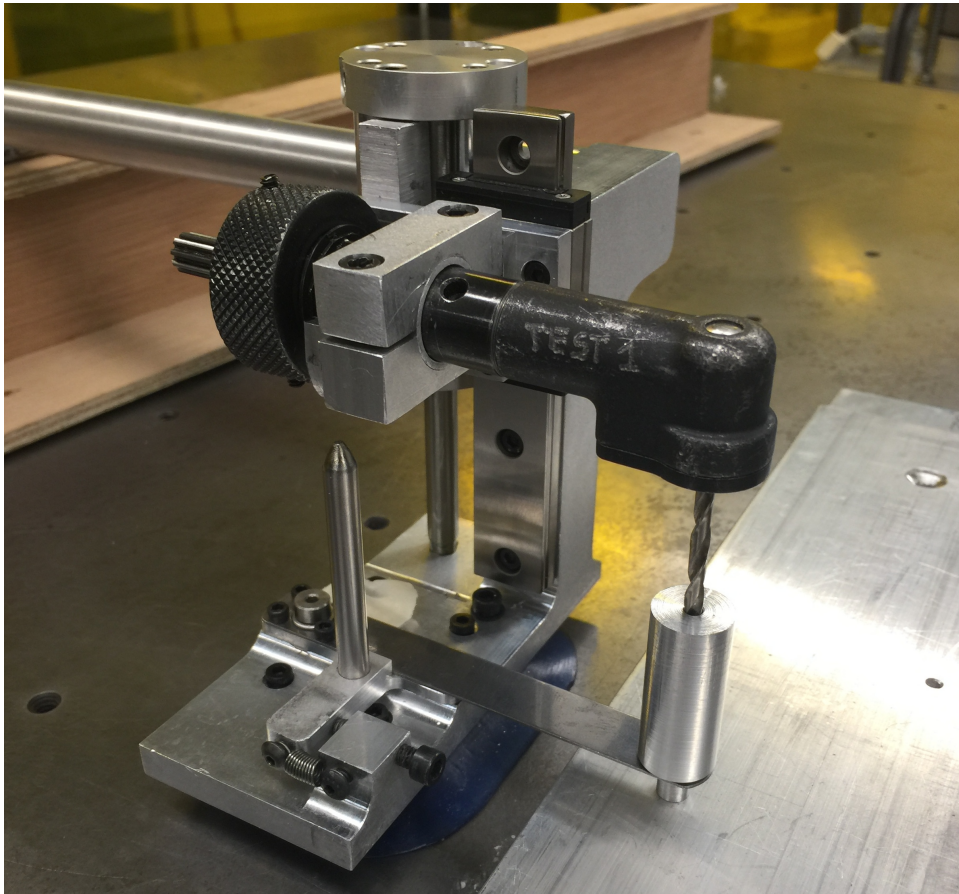


Figure 3.12: The manually operated pneumatic tool drill system being aligned with the alignment device.

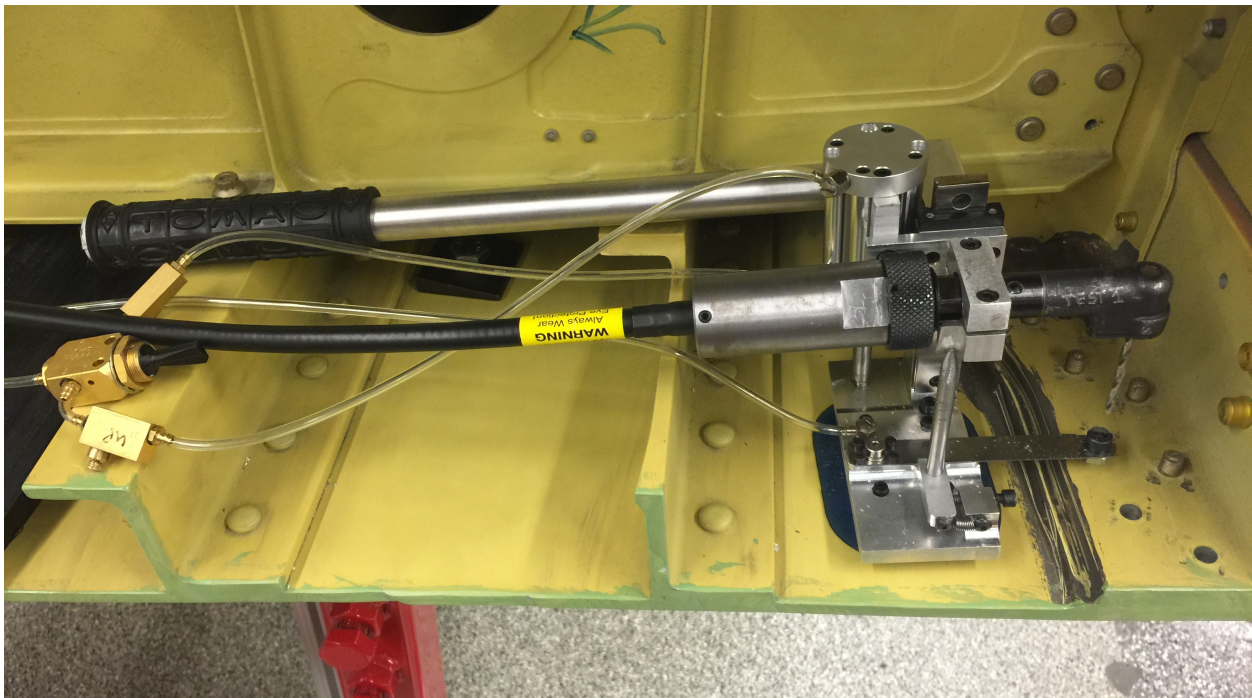


Figure 3.13: The manually operated pneumatic tool being placed in the cross-section of an actual airplane wing. Note that a wedge would be inserted between the handle and the last stringer it spans.

This alignment device would eventually prove useful for the final design. However the final drill design ends up looking, any design that includes a locator pin will likely need an alignment tool to ensure accuracy.

### 3.5.5 Operating Procedure

The operating procedure for the manually operated pneumatic tool during the testing phase was as follows:

1. The operator holds the system by the handle, inserts it through the access hole, and sets it near the spar chord flange at the end of the bay. At this point, the operator uses the handle to drag the locator pin across the spar chord to identify pilot holes.

2. After a pilot hole has been located by the locator pin, the operator turns on the vacuum pad, securing the system to the wing skin.
3. At this point there is an additional step that was discovered to be necessary after preliminary testing. The operator should insert a wedge or other support between the system handle and one of the stringers that the handle spans. This will provide a reaction for the moment that will be caused by the drill force, and prevent the system from rotating about the suction pad.
4. Next, the operator turns on the air motor, which drives the drill spindle via the flexible drive shaft.
5. While the drill is running, air is diverted to the bottom of the air cylinder, causing the drill spindle to descend downward in the vertical  $z$ -direction. The drill bit will enter the pilot hole, and begin to drill into the surface below while the air cylinder continues to provide downward force, which is reacted through the suction pad.
6. Once the hole has been drilled through the entire surface, the operator flips the air switch to make the drill spindle rise again, and then shuts off the air motor, ending the rotation of the drill spindle. At this point, the operator turns off the suction pad, grabs the handle, and begins locating the next pilot hole in the same spar chord. The process is repeated until all of the holes in the spar chord are back-drilled, at which point the operator will move the system to the other end of the same bay, or to a new bay entirely.

It is instructive to note that future design iterations will not require this many steps. The final system will likely have only one switch for the operator to engage, and all of the following steps would be automatic.

## Chapter 4

### PROTOTYPE TESTING

After the pneumatic tool prototype was completed, tests were designed to quantify whether the system would be a sufficient replacement for the current mode of operations. These tests were intended to determine the position accuracy and diameter uniformity of holes drilled by the manually operated pneumatic tool, and would determine the operational timing. The tests would also determine the maximum errors that would prevent rework. The results informed design recommendations for future systems.

#### **4.1 Test Bench**

A test bench was designed and manufactured to simulate the conditions within the confines of the wing. The purpose of the test bench was to see where the design succeeded, and more importantly where it fell short.

This test bench was built with the adjustability to simulate the dimensions of all the bays that were being considered. These included:

- Vary the distance of the stringer to the spar chord.
- Vary the stringer to spar chord height.
- Incorporate obstructions such as stiffeners and slat cans.
- Include and remove stringer run out.
- Vary the height of the ceiling and upper stringers.

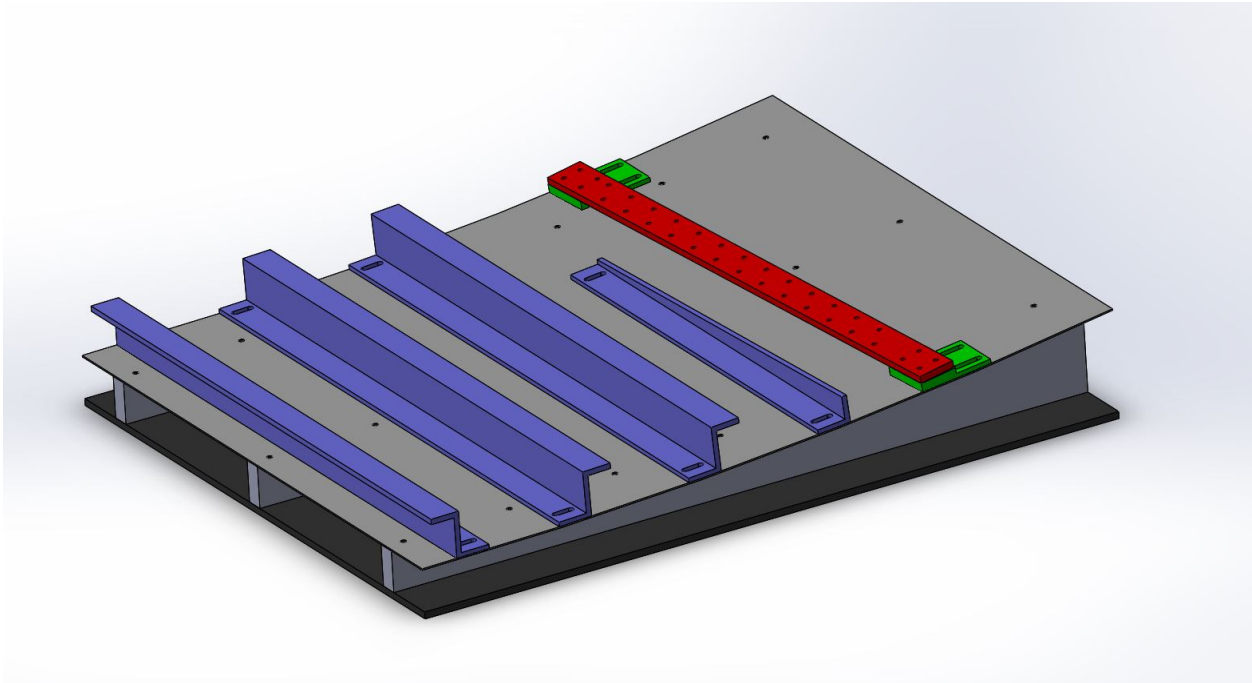


Figure 4.1: The test bench design in CAD.

## 4.2 *Offset Drill Test*

Earlier it was discussed that unless the system was sufficiently compliant, there would be an unavoidable position error between the actual drill placement and the pilot hole.<sup>1</sup> It was decided that creating a compliant system to correct for this error would be unnecessarily complex. This led to the question of whether or not the resulting error would be acceptable.

The purpose of the back-drilling procedure is to extend the interior pilot hole through the surface of the wing to provide a new pilot hole on the outside surface. This new pilot hole will be used to locate the final hole.

Since this system is designed to drill pilot holes for a larger hole, it follows that the drill placement can have some level of allowable error before any overlap between the hole perimeters is observed. This test is intended to determine what error is allowable, and

---

<sup>1</sup>See section 3.3.4.

whether the system meets that criteria.

Currently, the back-drilling procedure is completed by hand. Since the human hand is compliant, once the operator of the drill has found the pilot hole, they can fairly accurately insert the drill bit into the pilot hole, and complete the back-drilling procedure.

However, this is not the case for a mechanical back-drilling device. A mechanical system will locate the pilot hole, and then proceed to lower the drill bit into the hole. However, the drill bit will rarely be perfectly in line with the pilot hole, and will experience some positioning error. If that error is fairly small, the pointed end of the drill bit will drive the drill into the pilot hole, and the hole will be completed. This raises a question: how far from the true pilot hole position can the drill be, and still create a satisfactory pilot hole?

The purpose of this test procedure is to answer that exact question.

Since the back-drilling procedure is merely used to create a pilot hole, there is more leeway in the amount of allowable error. It will not be the final procedure, since a larger hole will be drilled through the surface using this pilot hole for guidance. However, if the new hole is too far off the mark, there is the potential for the final hole to not entirely overlap with the original interior pilot hole, causing an overlap in the perimeters of the two holes. This error is referred to as the “snowman effect”, since the overlap of the two holes looks like a snowman, with two snowballs stacked on top of each other, as seen in figure 4.2.

The nominal goal for the  $x - y$  position error on these holes was defined to be .010”, with an acceptable value within .030” as defined by engineering. It is the one of the goals of this thesis to determine guidelines for how much error is acceptable for this task based on the geometry.

The back-drilled pilot hole is performed with a number 30 drill bit, which is .1285” in diameter. The final hole that will be drilled later will be performed with a .25” drill bit, which is almost twice the diameter of the pilot hole. Therefore, an equation is needed to calculate the allowable difference in the position of the pilot hole and the final hole to avoid the snowman effect.

For the purposes of this derivation, the diameter of the large final hole will be referred to

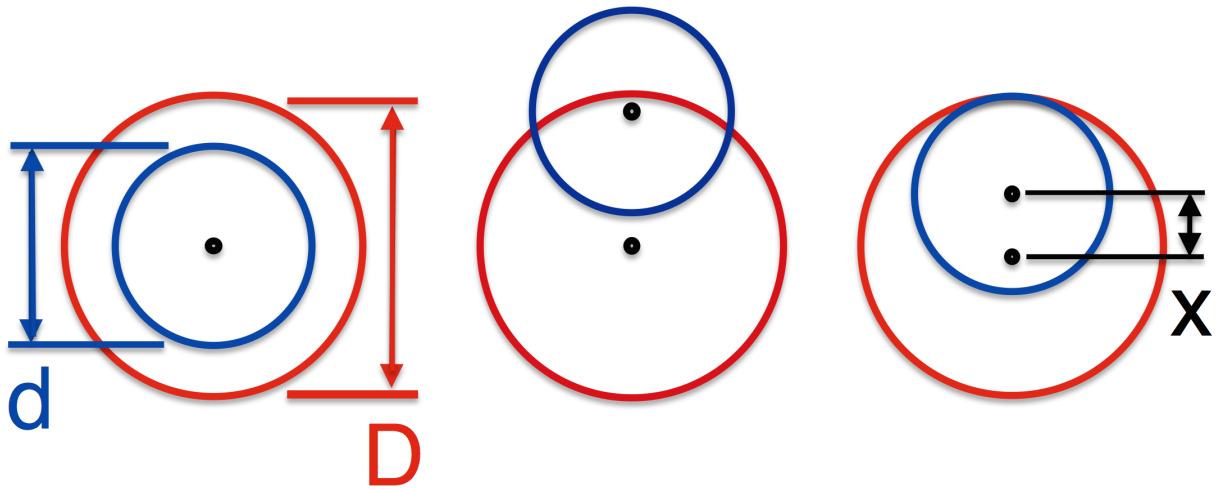


Figure 4.2: From left to right: the target hole configuration, a hole displaying the “snowman effect”, and a barely allowable hole. The smaller blue hole represents the back-drilled pilot hole, and the larger red hole represents the final hole.

as  $D$ , and the diameter of the back-drilled pilot hole will be referred to as  $d$ . The allowable difference between the centers of the two holes will be referred to as  $x$ , which is the variable that we intend to find. A graphic illustrating the geometry behind this derivation method can be seen in figure 4.2.

Additionally, for the purposes of this derivation, the surfaces on which the pilot hole and resulting exit hole appear are assumed to be parallel. This is not exactly true, but is a reasonable assumption for the majority of the wing bays. Final results will be slightly different when non-parallel drill surfaces are taken into account. The assumption is considered generally reasonable due to the small angle of difference and the thin nature of the surface.

If we set the two holes to intersect at their perimeter as in figure 4.2, then we can use the relationship between their diameters to find the difference between their centers,  $x$ :

$$1/2D = 1/2d + x$$

Rearrange to solve for  $x$ :

$$x = 1/2D - 1/2d$$

Enter the actual values for the diameters and solve:

$$x = .25''/2 - .1285''/2$$

$$x = .060''$$

As derived above, the maximum allowable error in the pilot hole is .060". Therefore, while the back-drilling procedure is performed, the exit hole must not be more than .060" different in position than the original pilot hole on the surface of the spar chord.

However, this error requirement only informs us of the allowable error on the *exit hole*. It does not inform us as to how close the device must position the drill bit to the original pilot hole on the surface of the spar chord inside the wing. The error of the exit hole could potentially be more or less than the initial error relative to the pilot hole, but is an unknown quantity until measured. To determine this allowable error, the following test was designed and performed on a programable three-axis mill:

1. A mill was used to drill six sets of fifteen pilot holes, each .25" deep.
2. Between the drilling of each hole, *Boelube*<sup>2</sup> was applied to the drill bit to ensure that the drill was properly lubricated, and the test was as uniform as possible.
3. The mill was then intentionally moved off-center of each row of pilot holes by increments of .005" before drilling through the entire surface. This resulted in six reference holes with no offset, six holes with a .005" offset, six holes with a .010", and so on, up to the last set of six holes, which will have a .070" offset.
4. The position of these holes was then measured relative to the reference holes. The difference between the position of each pilot hole and exit hole was compared and analyzed. Different orders of curves were fitted to the data and compared to each other.

An illustration of this offset drill test procedure is shown in figure 4.3

---

<sup>2</sup>*Boelube* is a solid lubricant that was developed by Boeing specifically for drilling applications.

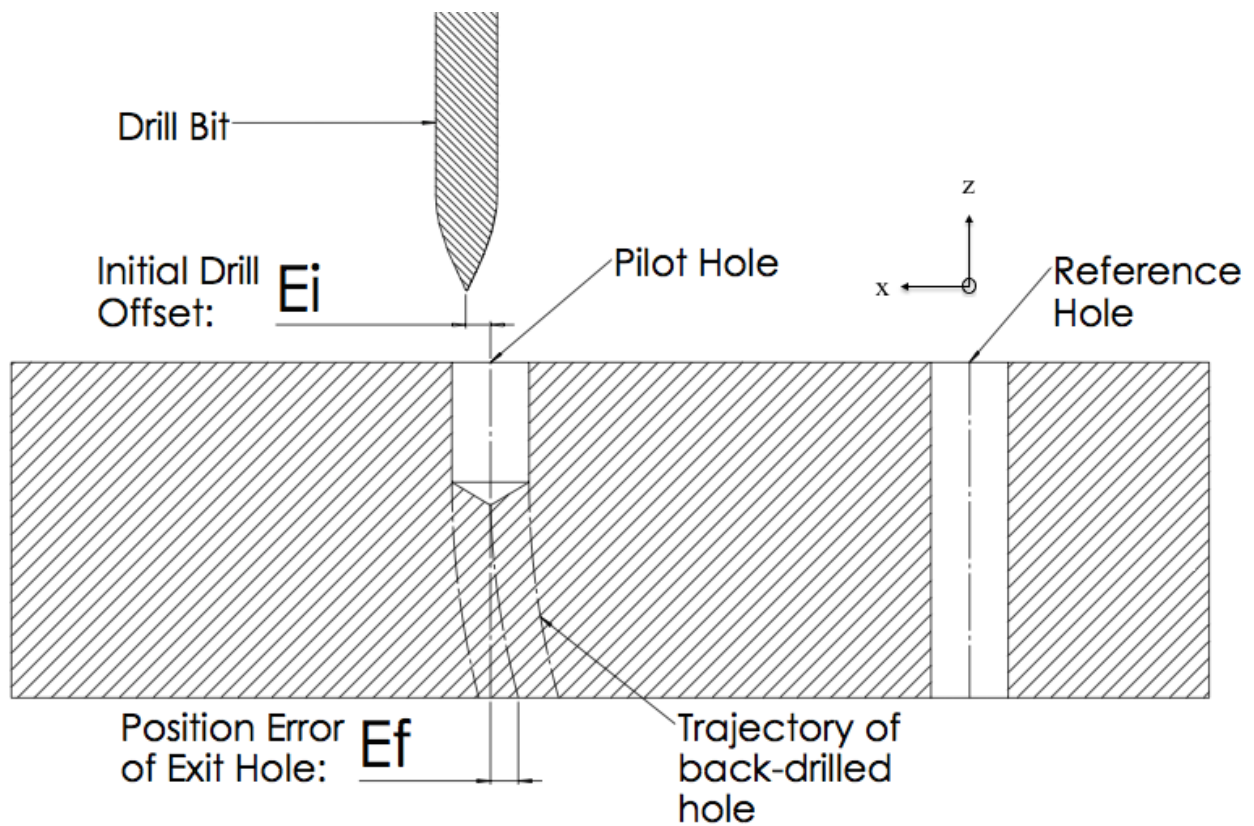


Figure 4.3: This illustration displays the offset drill test. The drill bit was intentionally offset from the pilot hole, resulting in a curved back-drilled hole. The position of the original pilot hole  $E_i$  and the final exit hole  $E_f$  were both compared to a reference hole, and the difference was defined to be the position error.

### 4.3 *Prototype Testing*

This test was intended to verify the manually operated pneumatic tool. The device was utilized to drill a number of holes, and three different sets of data were gathered to determine the practicality of the system. The following data sets were gathered during and after the prototype drill test:

- **Position Error Data:** This data set was intended to determine how much position inaccuracy is typically observed with this new drill system. After the entire drill test was performed, each exit hole was compared to the respective pilot hole to see how far off the system typically drills. Then this data was compared to the allowable error estimated from the offset drill test to determine whether this pneumatic tool is sufficient.
- **Timing Data:** This data set was intended to determine the typical time required for the new system to drill a series of holes. While the hole test was being performed, it was timed. This time was recorded for several holes, averaged, and evaluated compared to manual operator time.
- **Hole Quality Data:** This data set was intended to determine the typical hole quality that results from the use of this new system. The diameter of each hole was measured with a “split-ball gauge” in both the  $x$ -direction and the  $y$ -direction. These diameter measurements in each direction were compared to determine how cylindrical the hole is, to ensure that the holes were not excessively elliptical. Additionally, this diameter data provided evidence as to the predictability and uniformity of the holes that this pneumatic tool typically drills.

The following list describes the intended testing procedure for this prototype test.

1. A programable three-axis mill was used to drill pilot holes .25” deep on a .7” thick piece of aluminum.

2. Each hole was completed with the suction-pad drill system, as placed by hand utilizing the locator pin.
3. The time required to complete the drilling operation for a specified series of holes was recorded. This was the “timing” data set.
4. The original known distance between each pilot hole with the measured distance between each new exit hole were compared. This was the “position error” data set.
5. The maximum and minimum diameter of each hole were measured. This was the “hole quality” data set.
6. The hole data and timing results were analyzed and quantified to determine if the holes were sufficient.

## Chapter 5

# EVALUATION

### 5.1 *Offset Drill Test Results*

The offset drill test was found to have remarkably uniform results. As can be seen from the cross-section in figure 5.1, the holes start out perpendicular to the surface, and eventually diverge until they are substantially curved relative to the entrance and exit of the hole. This figure illustrates that for greater offset values, there can be observed a substantial difference between the position of the entrance hole at the top and the exit hole at the bottom.

As described in chapter 4, six sets of fifteen holes each were drilled, with increasing offset error from zero to seventy thousandths of an inch.

Figure 5.2 illustrates the results. The relationship between the imposed initial offset error and the final position error of the exit hole was found to be nearly linear. The error bars illustrate that the data was fairly uniform without any significant outliers. In all cases, the observed position error of the exit hole was *less* than the imposed offset error at the pilot hole.

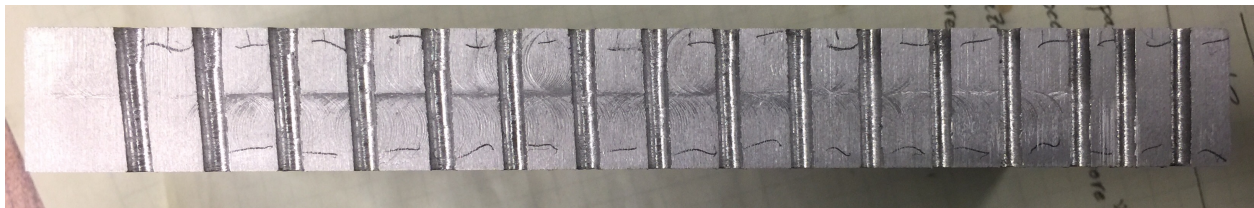


Figure 5.1: A cross section of the completed offset drill test. Note that the holes toward the right side of the image descend fairly straight through the surface, while as the holes approach the left, they become more and more slanted relative to the surface. This is due to the increasing drill offset from right to left.

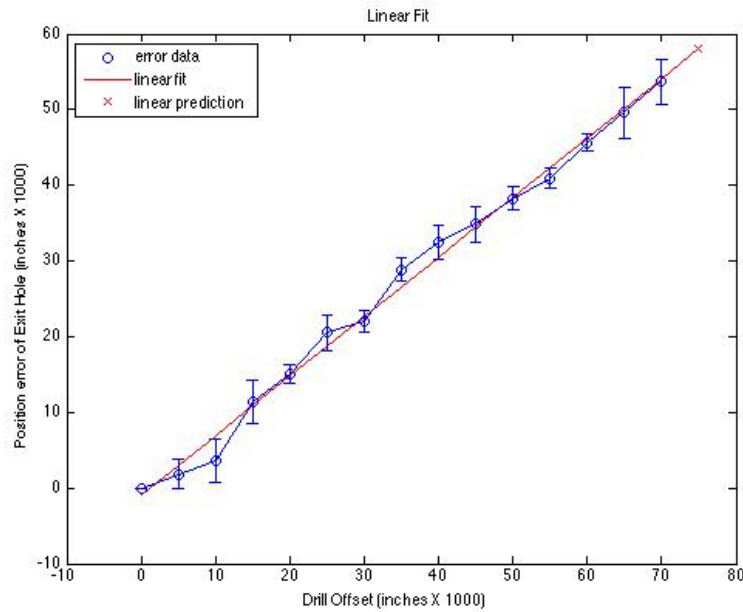


Figure 5.2: This graph displays the position error observed relative to the offset error imposed, and the best fit line.

The figure also displays the best fit line through the analyzed data. Several different orders of lines were fitted to the data, including a linear line, a quadratic, a cubic, and a fourth order line. Of the various orders of line that were fitted, the linear line was determined to be a sufficient solution and provided the most reasonable prediction for extrapolated results. As can be observed, there are no significant outliers in the data, and the line fits the general trend remarkably well. The equation for the line was:

$$Ef = .7849 Ei - .8875$$

Where  $Ei$  represents the initial position error relative to the pilot hole, and  $Ef$  represents the final position error of the exit hole relative to the original pilot hole. The units are in thousandths of an inch.

Note that the slope of this line is less than one. Based on this line, the position error of the exit hole will always be a lower value than the initial drill offset.

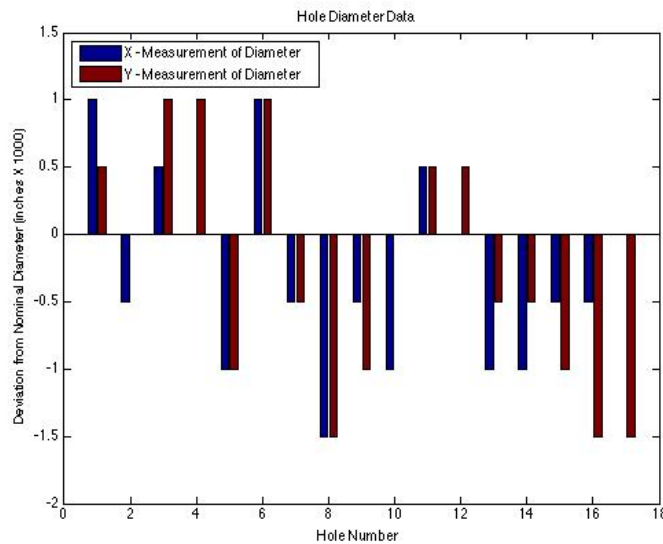


Figure 5.3: This graph displays the diameter deviations from the mean, measured in the  $x$  and  $y$  directions.

## 5.2 Prototype Test Results

### 5.2.1 Diameter Data

The prototype test results are displayed in figure 5.3. The diameter ranged from .127” to .1295” with an average diameter of .1282”. These results display holes with no significant tendency toward an elliptical cross section. If there were a tendency toward elliptical holes, the data would display significant differences between the  $x$  and  $y$  diameter measurements. Instead, the  $x$  and  $y$  diameter measurements tend to appear in pairs, with similar values.

### 5.2.2 Position Error Data

The position error data gathered from the prototype test remained within the allowable error. The position error data ranged from -.014” to +.026”, with an average error in the  $x$  direction of +.012” and an average error in the  $y$  direction of -.005”. These errors are plotted in figure 5.4. Recall that the maximum allowable error determined in section 4.3.1

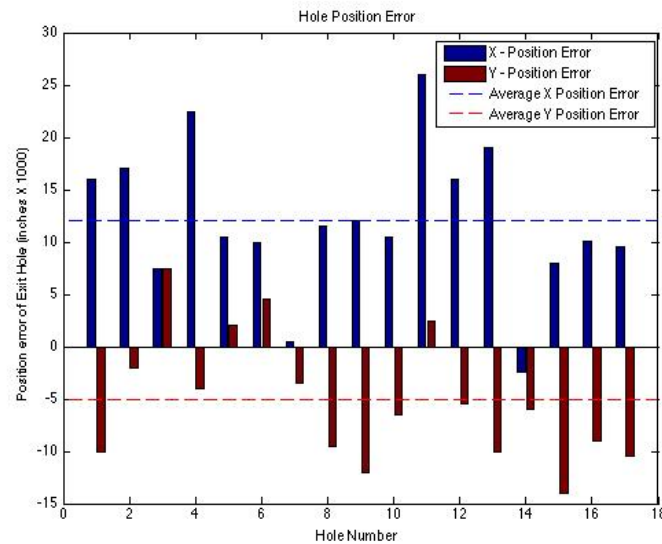


Figure 5.4: This graph displays the position error data. The  $x$  - direction was defined as away from the drill, and the  $y$  - direction was defined as to the left of the drill. Note that the average  $x$  error is significantly more than the average  $y$  error, and consistently positive.

was .060" from geometry, with a goal of .010", with acceptable errors within .030". The observed position error from the prototype test was less than half of the calculated allowable error, and just barely within the acceptable error. The average error in the  $x$  and  $y$  directions are close to the nominal error goal of .010".

### 5.2.3 Timing Data

The average cycle time for the back-drilling process was found to be 45 seconds. This includes the use of the locator pin to position the system, and the time to set up and secure the drill to the surface.

Of the 45 second cycle time, 33 seconds of that time was consumed by the actual back-drilling process. It took 12 seconds for the positioning and set up of the pneumatic tool.

## Chapter 6

# CONCLUSIONS

### 6.1 Discussion of Results

#### 6.1.1 Offset Drill Test and Allowable Error

Based on the offset drill test results, it was determined that the maximum allowable position error for the back-drilling procedure to prevent rework and avoid the “snowman effect” was .060”. This is twice the value of .030” considered acceptable by engineering, and six times the nominal goal of .010”.

It was also found that the relationship between the initial position error for the drill and the resulting final exit hole was linear. The best fit line resulted in an equation with a slope that was *less than one*. This indicates that regardless of the error performed by the pneumatic tool in locating the pilot hole, the resulting back-drilled hole will have an error that is *less* than the initial locator error.

#### 6.1.2 Prototype Position Error

Based on the prototype drill test performed with the manually operated pneumatic tool, it was found that the average position error was .012” in the  $x$  - direction and -.005” in the  $y$  - direction. These average errors are roughly one third of the acceptable error of .030”, and close to the nominal error goal of .010”. The maximum observed error in either direction was .026”, which is just barely within the range of acceptable error.

However, these test results present new questions. Why is the position error in the  $x$  - direction so biased in the positive  $x$  -direction? Why is the average error in the  $x$  - direction more than twice the average error in the  $y$  - direction?

It is speculated that the act of engaging the suction cup may pull the system slightly backward from the initial position located by the locator pin. When the locator pin initially positions the drill system, the suction cup is not engaged, and the system is free to move as the operator intends. Once the operator has located the hole and engages the suction cup, the system is pulled downward, closer to the wing surface. During this slight downward motion, the locator pin is still engaged in the hole, and pushes the system backward slightly. This process was observed in video playback of the drilling operation. This could potentially account for the larger and consistently positive error in the  $x$  - direction.

The average error in the  $y$  - direction is smaller, and roughly half the nominal goal of .010". However, this error was observed to tend in the negative direction. This result may be due to an error during the alignment of the drill system with the locator pin.

It is important to note that the allowable error and the graph relating initial offset to exit hole position error were calculated for a pilot hole .25" deep and a total material depth of .7", under the assumption that the interior and exterior surfaces were parallel. In some locations, the spar chord flange and the wing skin are out of parallel with each other by up to 1.5 degrees. This could lead to additional error of up to .017".

### *6.1.3 Prototype Diameter Error*

The maximum and minimum diameters ranged .0025".

Part of the motivation for designing the manually operated pneumatic tool stemmed from challenges encountered during preliminary testing of the five-axis drill platform. The cantilever arm of the drill platform allowed too much bending to take place during drilling, and created elliptical holes. The pneumatic tool solved this problem by providing a secure suction cup to offset the drill force, and a reaction for the moment through the use of the wedge between the handle and the stringer.

#### *6.1.4 Prototype Cycle Time*

The timing results need to be considered in two separate categories: the time required to position and align the mechanism, and the time required for the drilling function.

The average time to complete each back-drilling operation was found to be 45 seconds. However, 73 percent of this time was the function of drilling the hole. The functions of positioning the drill, aligning to the pilot hole with the locator pin, and engaging the suction cup took 27 percent of the time.

The cycle time may have been compromised by the fatiguing flexible drive shaft. It is speculated that a more durable flexible drive shaft could improve cycle time by providing more torque and drill speed.

Only 27 percent of the cycle time was consumed by positioning the mechanism. These data suggest that the locator pin is a practical method for aligning to pilot holes.

## **6.2 Implications of Research**

The original motivation behind this research revolved around the goal to increase the rate of production for commercial airliners. The research goals were to design a mechanical system capable of drilling satisfactory holes within the confines of a wing bay with minimal human interaction. Ideally, this system would reduce the cycle time for completing back-drilled holes.

Initially, this research project focused on the ideal of creating a completely independent device that could maneuver within the confines of the wing, and access many different hole locations. However, as the research progressed, more human interaction was deemed necessary to create a viable first system.

Due to the space constraints in the wing, an actual mobile crawler was tabled for future projects, and a five-axis drill platform was designed and constructed that would be placed by hand within a wing bay. This system would remain stationary as placed by the operator, but the five-axis arm system was designed to allow it to reach the majority of hole locations

within a given wing bay.

Due to preliminary test results, several challenges were identified with the five-axis drill platform. It was too large for most of the wing bays, and the extensive length of the arm allowed an excessive amount of bending during drill operations, resulting in poor hole quality.

The five-axis drill platform design has not been dispensed with. It was understood from the beginning of this research project that any resulting design would merely be the first iteration among several generations of design evolution. A new version of the five-axis platform is currently under design by other researchers. Eventually, a modified version of the pneumatic tool could be implemented as an end-effector for future platform designs.

However, it was recognized that regardless of the quality of new design improvements for the five-axis drill platform, it would never be able to reach the smaller bays toward the tip of the wing. A smaller system would need to be designed for this specific task, and again, more human interaction was deemed necessary. To reduce the size of the system further, the goal of independently accessing all hole positions within the wing bay was abandoned. This new system would only drill one hole at a time, and would need to be maneuvered and positioned by an operator. This new design proposal was still seen as an improvement over the current mode of operation, since the mechanic would not have to personally climb or reach within the confines of the wing due to the presence of a substantial handle.

This new system was designed and constructed, and deemed the “manually operated pneumatic tool”. It was entirely air powered, and utilized a suction cup to secure to the wing surface and offset drill force. It also employed the use of a “locator arm” that would allow the operator to locate holes through tactile feedback.

Small design changes were made to the pneumatic tool after preliminary testing, and final tests were performed. The system meets or exceeds all criteria that it was evaluated for. Challenges were still encountered, and a substantial list of design improvements has been prepared in section 6.3 on the following pages.

Several specific conclusions can be drawn from these test results, as follows:

- The drill system does not have to perfectly align with the pilot hole. An error in position of .060" will prevent rework errors, and an error of .030" is acceptable.
- Any error between the placement of the drill and the pilot hole will result in a *lower* error in the position of the resulting exit hole.
- The manually operated pneumatic tool drills holes that are within the calculated allowable error. The maximum position error for an exit hole was .026", which is slightly less than the acceptable value of .030" for the allowable error. However, it was observed that the error in the  $x$  - direction was significantly biased away from the drill system, which suggests a mechanical flaw.
- The manually operated pneumatic tool drills holes that are satisfactory in shape and dimension. The diameter of the holes range .0025", and there is no significant tendency toward elliptical hole shape.
- The test results for the pneumatic tool suggest the locator pin is a practical method for locating pilot holes and positioning the drill.
- The use of the flexible drive shaft reduced the weight of the system but eventually fatigued and failed. A more sturdy version is recommended for future design iterations.
- The suction cup employed for final testing was sufficient for back-drilling operations.
- The cycle time of the system for back-drilling holes was found to 45 seconds, which is comparable to the cycle time for manual operation. Drilling could potentially be sped up through the use of a larger air cylinder for downward force and the application of a sturdier flexible drive shaft.

### **6.3 Future Design Improvements**

It was always understood that this prototype would not enter the factory floor, and would merely be the first generation in an evolution of several designs. It is important whilst evaluating this system to keep in mind new ideas and potential improvements to assist in the design of generation II.

#### *6.3.1 Height*

The first general improvement that will need to be considered is overall dimensions. The smaller the system can get, especially in height, the more wing bays it will be capable of accessing. This was always one of the top design constraints and considerations, and should remain so moving forward.

Height is the most critical challenge, and the hardest to reduce further. All manners of reducing height should be explored, including finding lower profile suction cups, designing a lower profile base plate, or making the suction cup itself the base plate.

#### *6.3.2 Locator Pin*

One of the challenging aspects of this system to operate in practicality was the locator pin. The theory behind the locator pin was that it should make it easier for the operator to locate pilot holes, since it would provide sensory feedback. In reality, the final design of the locator pin was mounted too high. It did not press hard enough into the testing surface, and interfered with the drilling operation and needed to be manually pushed aside during drilling.

The locator pin should be mounted lower; much closer to the spar chord surface. It should be entirely out of the path of the drill bit by the time the drill bit descends to the pilot hole. In fact, it should be mounted *below* the lowest point of the spar chord surface. This is because it is designed as a cantilever spring, and gives better feedback when the spring is under load. This cantilever spring should be stiffly engaged throughout the entire

process of locating the hole and securing the suction cup.

The locator pin is suspected as the main culprit in the position error data that was biased in the positive x - direction. The locator pin should be much stiffer than the current model, and design changes need to be made to ensure it will still perform on multiple spar chord heights.

Ideally, the locator pin should include a locking mechanism. As mentioned earlier, the locator pin was initially fairly floppy, and would slide to the side with a small amount of force, preventing it from being useful for locating pilot holes. Fortunately, the change made by using a stronger spring made this much less of an issue, and the locator pin managed to locate the pilot holes without much trouble during actual testing. However, it is recommended that the next version of the design incorporate some form of locking mechanism to ensure that it is in the right configuration when locating pilot holes for drilling.

### 6.3.3 Drill Spindle Configuration

While the drill spindle worked well during testing, it was recognized that the mounting configuration would need to be modified to allow the system to operate in more of the wing bays. Many of the wing bays include a stringer that is too close to the spar chord to allow the drill spindle to descend to the wing surface in its present configuration, due to the rear-facing nature of the flexible drive shaft adapter.

It is proposed that a sideways facing drill spindle would be superior for reaching these unique wing bays, and would still work in the other wing bays. With this configuration, the drill spindle would be mounted further forward, and turned 90 degrees, such that it is parallel to the spar chord, as in figure 6.1 (b). Additionally, the entire tool could be turned 90 degrees and mounted directly on the spar chord flange as shown in figure 6.1 (c).

While this new concept for drill spindle placement would allow the system to reach more bays, it still presents a challenge not present in the original design: the new configuration is incapable of drilling holes in *both* the right and left halves of the same spar chord.

There are two possible solutions to this dilemma. First, the drill spindle could be rear-

ranged on the system during work in each bay. However, calibrating the drill is not a trivial task, and rearranging and recalibrating the drill every few minutes would be impractical due to the time constraints present in the assembly environment. The second solution is that each back-drilling crew be supplied with *two* of these manually operated pneumatic tools, one with a right facing drill, and the other with a left facing drill. Considering the time savings that could be achieved by accessing more bays and not frequently recalibrating the drill, the cost of supplying each crew with two drill systems seems appropriate.

#### 6.3.4 *Suction Cup*

The commercial suction cup that was incorporated after preliminary testing proved sufficient to offset the drilling procedure. However, there were two challenges with the suction cup.

First, the compliance of the suction cup allowed it to tilt backward during the drilling operation, which required the use of a wedge between the handle and a stringer. Future design iterations will need to address this issue by offsetting this drill moment in another fashion. Potential solutions include changing the drill configuration as mentioned previously, or implementing a stabilization foot to offset the moment.

Additionally, the drill positioning results were significantly biased in the positive x-direction, and the suction cup was seen as the primary culprit. When the vacuum is engaged, the suction cup pulls the drill system downward in the z-direction toward the skin. This change in vertical position results in a corresponding change in the x position of the device. The next iteration will need to address this issue. One potential solution would be a lower profile suction cup that does not change position when the vacuum is engaged.

#### 6.3.5 *Damper*

It was discussed during later design changes that a damper should be incorporated to control the speed of the downward z-axis motion of the drill spindle during drilling. Such a damper was never implemented due to time constraints, and the speed of the final system was partially controlled by adjusting the volume of the air entering the air cylinder.

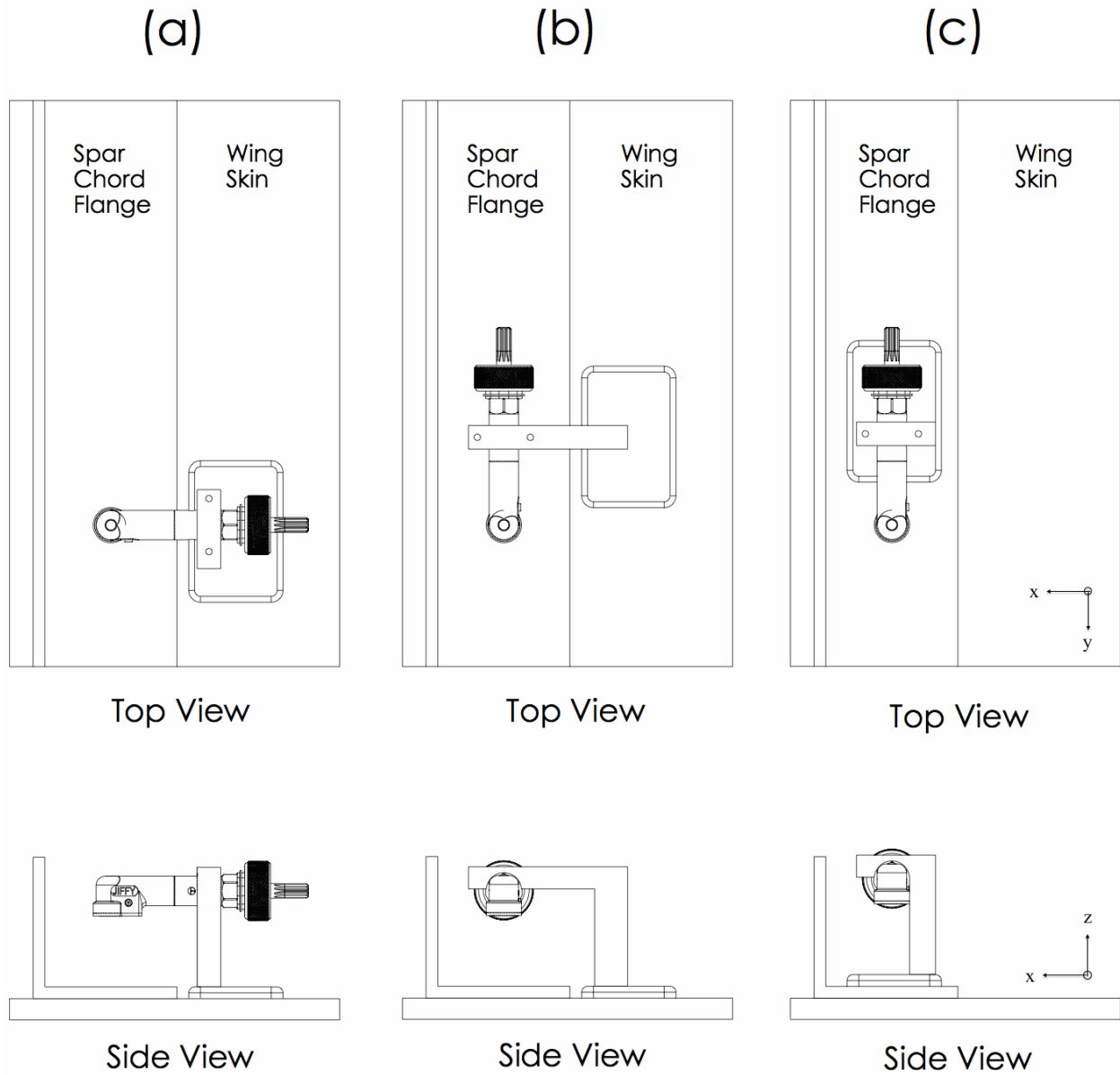


Figure 6.1: These images display various options for the drill spindle configuration. (a) shows the configuration of the prototype that was tested for this thesis. (b) shows a new configuration where the suction cup still secures to the skin, but the drill spindle is now parallel to the spar. (c) shows a new configuration where the suction cup secures to the spar chord flange, while the drill spindle is parallel to the spar.

While adjusting the air volume appears to have been sufficient in controlling the speed of this design, it is proposed that a damper be incorporated into future designs to ensure more control over the speed of the drill. Additionally, reducing the volume of the air is not an ideal manner in which to control speed, since it reduces the available power for drilling. This is another reason why a damper is recommended.

### *6.3.6 Flexible Drive Shaft*

During preliminary tests, the flexible drive shaft eventually fatigued and failed. The shaft was severed internally near the base, where the coupling attached to the drill motor.

During most of the actual drill testing, the flexible drive shaft did not appear to be stressed. However, stress on the flexible drive shaft was observed to increase during the last portion of drilling, as the back surface of the test piece was broken through. This “breakthrough” portion of the drilling procedure would frequently cause the drill to slow down, and the flexible drive shaft to wind up on itself, initiating fatigue.

It is recommended that a more sturdy flexible drive shaft be chosen for the next version of the pneumatic tool design. This flexible drive shaft was more than flexible enough for the drill procedures, and a substantially stiffer shaft could be chosen without losing the advantages of a flexible shaft. The system clearly needs to be more redundant in the future. A stiffer shaft would not only make the system more durable, but would likely improve the cycle time by providing more power and torque to the drill spindle.

### *6.3.7 Multiple Design Configurations*

Eventually, it is intended that this system will evolve into two different forms. One device that remains manually operated for the smallest wing bays, and another device that is customized to act as a drilling end-effector for future iterations of the five-axis platform in larger wing bays. If implemented on the end of the five-axis arm, the suction cup would eliminate the bending cantilever.

## BIBLIOGRAPHY

- [1] The Boeing Company  
<http://www.boeing.com>
- [2] Martin Udengaard, Karl Iagnemma. *Analysis, Design, and Control of an Omnidirectional Mobile Robot in Rough Terrain*. Journal of Mechanical Design, Vol. 131, December 2009.
- [3] Haitao Liu, Tian Huang, Jianping Mei Xueman Zhao, Derek G. Chetwynd, Meng Li, S. Jack Hu. *Kinematic Design of a 5-DOF Hybrid Robot with Large Workspace/Limb-Stroke Ratio*. Journal of Mechanical Design, Vol. 129, May 2007.
- [4] Hira Karagulle, Murat Akdag, Levent Malgaca. *A Mechatronic Design Process for Three Axis Serial Robots*. Proceedings of the ASME 2010 Biennial Conference on Engineering Systems Design and Analysis, July 2010.
- [5] Mathieu Baril, Thierry Laliberte, Clement Gosselin, Francois Routhier. *On the Design of a Mechanically Programmable Underactuated Anthropomorphic Prosthetic Gripper*. Journal of Mechanical Design, Vol. 135, December 2013.
- [6] Pinhas Ben-Tzvi, Andrew A. Goldenberg, Jean W. Zu. *Design and Analysis of a Hybrid Mobile Robot Mechanism With Compounded Locomotion and Manipulation Capability*. Journal of Mechanical Design, Vol. 130, July 2008.
- [7] Jane Shi, Brad Hamner, Reid Simmons, Sanjiv Singh. *Mobile Robotic Assembly on a Moving Vehicle*. Proceedings of the ASME/ISCIE 2012 International Symposium on Flexible Automation, June 2012.
- [8] Randy James, Basar Ozkan, Bahram Ravani. *Mechanical Design of a Robotic System for Automatic Installation of Magnetic Markers on the Roadway*. Journal of Mechanical Design, Vol. 128, March 2006.

## Appendix A

### ADDITIONAL FIGURES AND TABLES

This appendix is where you will find all of the figures, tables, graphs, matlab coding, and charts that were referenced elsewhere in this document or were otherwise relevant to the completion of this research.

#### ***A.1 Matlab Code and Graphs***

The data calculations were all performed in Matlab. The following pages include the Matlab code, raw data, graphs, and calculations performed for the test results.

#### ***A.2 Wing Bay Analysis***

Before design work could commence, the space constraints of the assembly environment needed to be fully understood. An extensive analysis was conducted of the wing model to quantify the dimensions of each bay. The following pages include the graphs that display this data.

#### ***A.3 Preliminary Design Analysis***

Pugh Charts for the preliminary design analysis are included on the following pages.

- [Introduction](#)
- [Enter Measured Hole Data](#)
- [Average Hole Data](#)
- [Plot visually](#)
- [Fit Lines to Data](#)
- [Plot Linear, Quadratic, Cubic, and 4th Order Fits](#)
- [Hole Quality Test for Hand-Placed End-Effector](#)

## Introduction

BARC @ UW

Offset Drill Test for Confined Space Back-Drilling Application

And Hole Quality Test for Hand-Placed End-Effector

Dec 15th, 2015 - Feb 24th 2016

Benjamin Janicki, Graduate Researcher

```
clc
clear all
close all
```

## Enter Measured Hole Data

```
% Hole entrance data - top of block
xt1 = [0 .2775 .6745 1.081 1.482 1.8775 2.28 2.682 3.084 3.483 3.8815 ...
       4.286 4.6835 5.079 5.482].';
xt2 = [0 .2755 .68 1.083 1.4815 1.8835 2.2845 2.6825 3.082 3.4815 3.889 ...
       4.293 4.6925 5.0855 5.489].';
xt3 = [0 .2775 .68 1.084 1.481 1.8855 2.2815 2.683 3.0885 3.488 3.887 ...
       4.291 4.692 5.0895 5.4965].';
xt4 = [0 .2785 .6775 1.082 1.483 1.884 2.2805 2.688 3.0855 3.487 3.885 ...
       4.286 4.6905 5.0945 5.4925].';
xt5 = [0 .2775 .681 1.087 1.482 1.885 2.2805 2.688 3.0935 3.49 3.885 ...
       4.279 4.6895 5.0895 5.493].';
xt6 = [0 .2785 .6805 1.0835 1.4855 1.886 2.28 2.684 3.086 3.489 3.889 ...
       4.291 4.6895 5.0935 5.493].';

% Hole exit data - bottom of block
xb1 = [0 .2735 .6715 1.0715 1.468 1.86 2.2575 2.6535 3.051 3.4545 3.8465 ...
       4.245 4.645 5.0355 5.4365].';
xb2 = [0 .273 .6755 1.068 1.4695 1.862 2.2595 2.6565 3.0545 3.453 3.846 ...
       4.248 4.643 5.0375 5.439].';
xb3 = [0 .278 .6785 1.077 1.4665 1.867 2.2585 2.6545 3.056 3.448 3.8505 ...
       4.2455 4.6425 5.043 5.432].';
xb4 = [0 .276 .6725 1.072 1.4665 1.862 2.2595 2.6555 3.052 3.453 3.848 ...
       4.2475 4.6445 5.038 5.44].';
xb5 = [0 .2765 .678 1.0725 1.466 1.863 2.2585 2.657 3.054 3.451 3.848 ...
       4.2465 4.6435 5.0365 5.439].';
xb6 = [0 .277 .6755 1.071 1.468 1.8645 2.2615 2.6575 3.057 3.45 3.848 ...
       4.248 4.645 5.0435 5.4375].';
```

## Average Hole Data

```

% Top average position of each hole: entrance
xt = (xt1 + xt2 + xt3 + xt4 + xt5 + xt6)/6;

% Bottom average position of each hole: exit
xb = (xb1 + xb2 + xb3 + xb4 + xb5 + xb6)/6;

% Define y axes for comparison
L = length(xt);
yt = zeros(L);
yb = ones(L)*-.7;

% Determine inconsistencies in data for error bars
XT = [xt1 xt2 xt3 xt4 xt5 xt6]*1000;
XB = [xb1 xb2 xb3 xb4 xb5 xb6]*1000;
N = 15;
ST = zeros(N,1);
SB = zeros(N,1);

for i = 1:N
    ST(i) = std(XT(i,:));
    SB(i) = std(XB(i,:));
end

```

### Plot visually

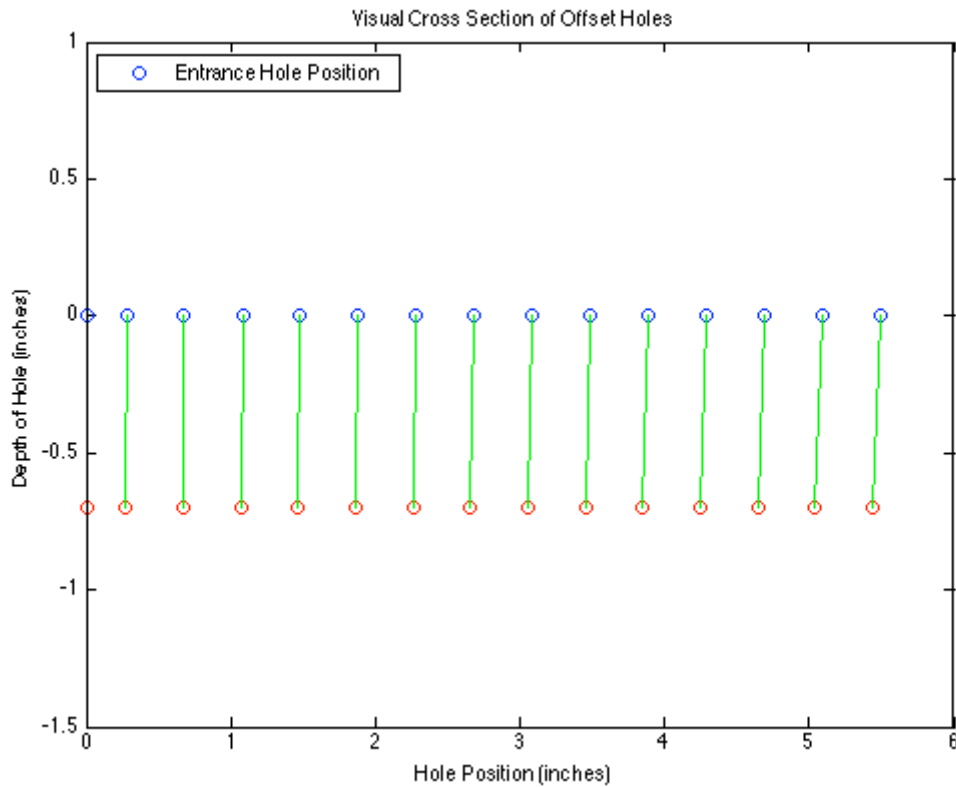
```

% Plot holes as they appear in cross-section
figure
plot(xt,yt,'bo',xb,yb,'ro')
hold on
xf = [0 0];
yf = [0 -.7];

for i = 1:L
    xf = [xt(i) xb(i)];
    plot(xf,yf,'g')
    hold on
end

axis([0,6,-1.5,1])
title('Visual Cross Section of Offset Holes')
xlabel('Hole Position (inches)')
ylabel('Depth of Hole (inches)')
legend('Entrance Hole Position','Location','NorthWest')

```



### Fit Lines to Data

```

% In thousandths of an inch
er = (xt - xb)*1000;
xr = (0:.005:.07)*1000;
xd = xr;
Nd = L;

% Compute polynomial coefficients:
for k = 2:Nd

    for i = 1:k;
        ANd(:,i) = xd.^(i-1);
    end

    % Polynomial Coefficients:
    ad(1:k,k-1) = ANd\er;

end

% Check the condition number:
Cd = cond(ANd)

% Note: This is a very big condition number, which is not ideal.
% However, as will be shown by the graph, the lines fit the data well.

del = xd(end) - xd(end-1);
w = [xd. '; (xd(end)+del)];

```

```

% Evaluate polynomials of each order:
for k = 1:Nd-1

    Pnew = 0;

    for j = 1:Nd-1
        Pnew = ad(j,k).*(w.^(j-1)) + Pnew;
    end

    Papprox(:,k) = Pnew;

end

% Y Data
Pactual = er;

% X Data
wreal = xd;

```

```

Warning: Rank deficient, rank = 7, tol = 2.2857e+00.
Warning: Rank deficient, rank = 7, tol = 1.5568e+02.
Warning: Rank deficient, rank = 6, tol = 1.0654e+04.
Warning: Rank deficient, rank = 6, tol = 7.3193e+05.
Warning: Rank deficient, rank = 6, tol = 5.0438e+07.
Warning: Rank deficient, rank = 6, tol = 3.4844e+09.
Warning: Matrix is close to singular or badly scaled.
         Results may be inaccurate. RCOND = 5.393778e-29.

```

```
Cd =
```

```
2.7161e+26
```

### Plot Linear, Quadratic, Cubic, and 4th Order Fits

```

figure
plot(wreal,Pactual,'ro')
hold on
plot(w,Papprox(:,1),'b',w(end),Papprox(end,1),'bx')
hold on
plot(w,Papprox(:,2),'c',w(end),Papprox(end,2),'cx')
hold on
plot(w,Papprox(:,3),'g',w(end),Papprox(end,3),'gx')
hold on
plot(w,Papprox(:,4),'m',w(end),Papprox(end,4),'mx')
title('Least Squares Fit')
xlabel('Drill Offset (inches X 1000)')
ylabel('Position error of Exit Hole (inches X 1000)')
legend('error data','linear fit','linear prediction','quadratic fit',...
       'quadratic prediction','cubic fit','cubic prediction',...
       '4th order','4th order prediction','Location','NorthWest')

% Notes:

```

```
% All fits are good. Linear, Quadratic, and Cubic fits all make reasonable
% predictions for future data. The forth order fit gives a less reasonable
% prediction for future data.
% Based on the data and graph, it is assumed that linear is the best fit.

% Show Linear Graph alone with error bars
figure
plot(wreal,Pactual,'bo')
hold on
plot(w,Papprox(:,1),'r',w(end),Papprox(end,1),'rx')
hold on
errorbar(xr,er,SB,'b')
title('Linear Fit')
xlabel('Drill Offset (inches X 1000)')
ylabel('Position error of Exit Hole (inches X 1000)')
legend('error data','linear fit','linear prediction','Location','NorthWest')

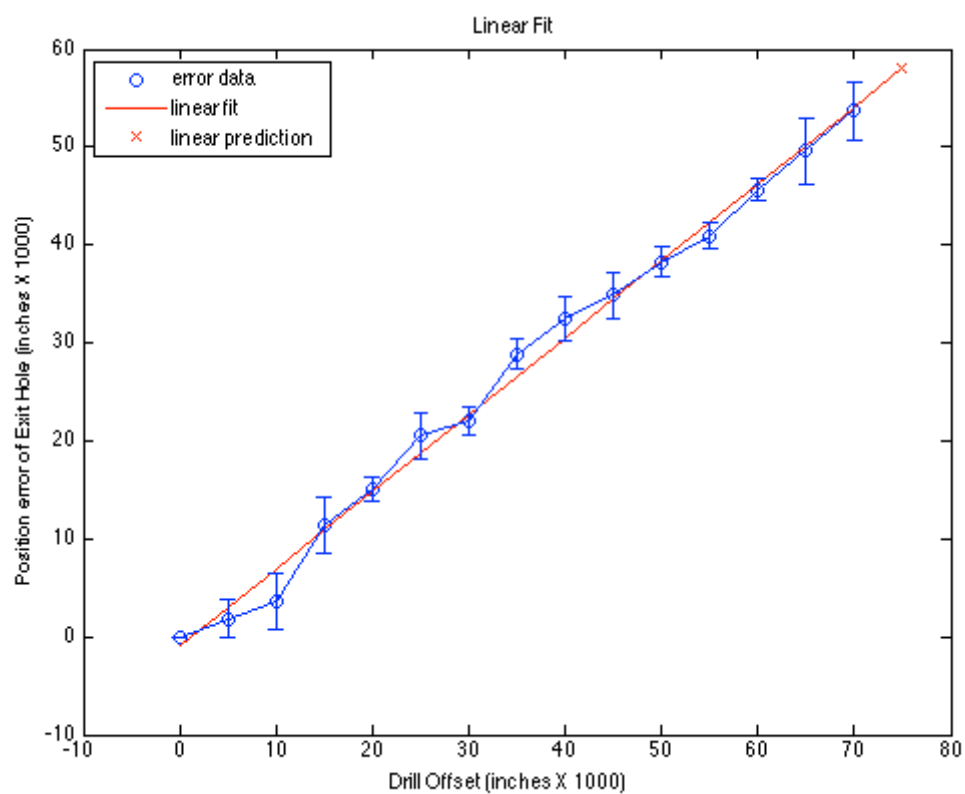
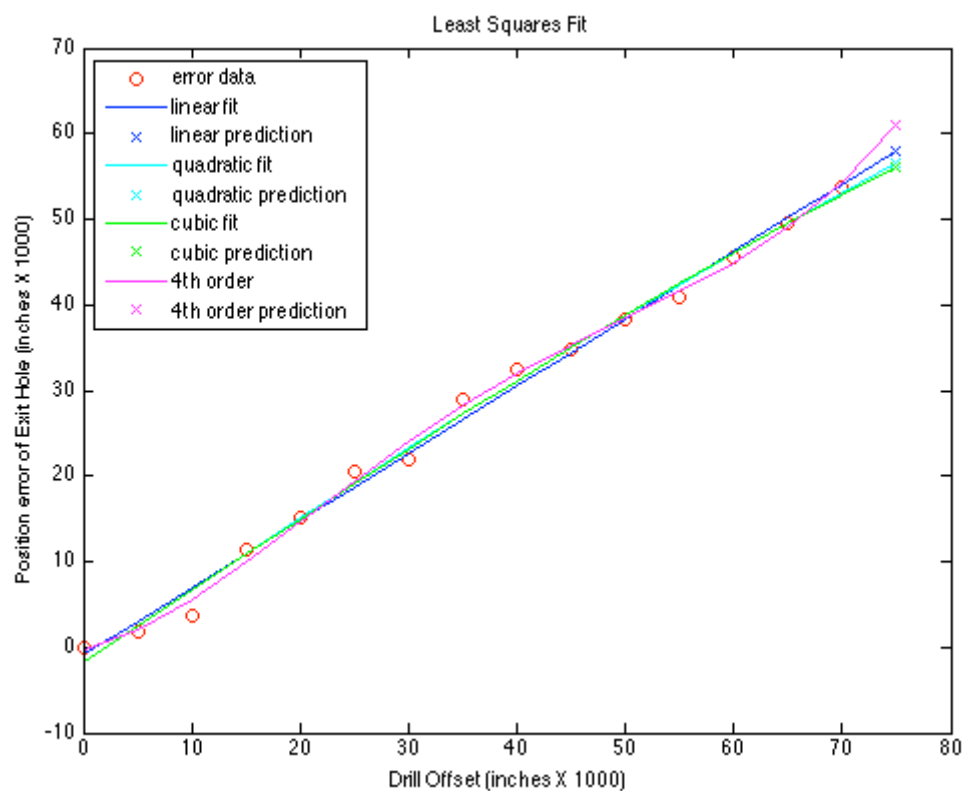
% Display the Slope and Y-intercept for the line
Slope = ad(2,1)
Yintercept = ad(1,1)
```

Slope =

0.7849

Yintercept =

-0.8875



### Hole Quality Test for Hand-Placed End-Effector

```

% X - Hole position entrance data - top
ht = [.942 .944 .9435 .944 .943 .945 .939 .9445 .9445 .943 ...
      .3425 .3425 .342 .3415 .342 .341 .342].';

% X - Hole position exit data - bottom
hb = [.926 .927 .936 .9215 .9325 .935 .9385 .933 .9325 .9325 ...
      .3165 .3265 .323 .344 .334 .331 .3325].';

% Y - Hole position entrance data - top
hty = [1.0765 1.479 1.89 2.279 2.68 3.0815 3.878 4.276 4.6785 5.0775 ...
       1.0815 1.48 1.88 2.281 2.68 3.08 3.4815].';

% Y - Hole position exit data - bottom
hby = [ 1.0865 1.481 1.8825 2.283 2.678 3.077 3.8815 4.2855 4.6905 5.084 ...
       1.079 1.4855 1.89 2.287 2.694 3.089 3.492].';

% Hole position error in thousandths
he = (ht-hb)*1000;
hye = (hty-hby)*1000;
hE = [he, hye]; % Combine into matrix to plot
hd = 1:length(he); % X-data on plot

% Average Error (thousandths)
avgEx = sum(he)/length(he)
avgEy = sum(hye)/length(hye)
MaxE = max(hE)
MinE = min(hE)

hv = [0,hd,18]; % (ensures that the dotted line crosses entire figure)
avEx = ones(length(hv),1)*avgEx;
avEy = ones(length(hv),1)*avgEy;

figure
bar(hd,hE,'grouped')
hold on
plot(hv,avEx,'b--',hv,avEy,'r--')
title('Hole Position Error')
xlabel('Hole Number')
ylabel('Position error of Exit Hole (inches X 1000)')
legend('X - Position Error','Y - Position Error',...
       'Average X Position Error','Average Y Position Error')

% Hole diameter data
dx = [.1295 .128 .129 .1285 .1275 .1295 .128 .127 .128 .1275 ...
      .129 .1285 .1275 .1275 .128 .128 .1285].';
dy = [.129 .1285 .1295 .1295 .1275 .1295 .128 .127 .1275 .1285 ...
      .129 .129 .128 .128 .1275 .127 .127].';

% Error between diameter directions
de = (dy - dx)*1000;
goal = ones(length(dx),1)*.1285;
dd = 1:length(dx);

% Deviation from nominal diameter
devX = dx - goal;

```

```
devY = dy - goal;
dev = [devX,devY]*1000;

figure
bar(dd,dev,'grouped')
title('Hole Diameter Data')
xlabel('Hole Number')
% axis([0 18 .125 .135])
ylabel('Deviation from Nominal Diameter (inches X 1000)')
legend('X - Measurement of Diameter','Y - Measurement of Diameter',...
       'Location','NorthWest')

% Find average, min, and max values
H = [dx;dy];
MinD = min(H)
MaxD = max(H)
AvgD = sum(H)/length(H)
```

```
avgEx =
```

```
12.0000
```

```
avgEy =
```

```
-5.0588
```

```
MaxE =
```

```
26.0000    7.5000
```

```
MinE =
```

```
-2.5000   -14.0000
```

```
MinD =
```

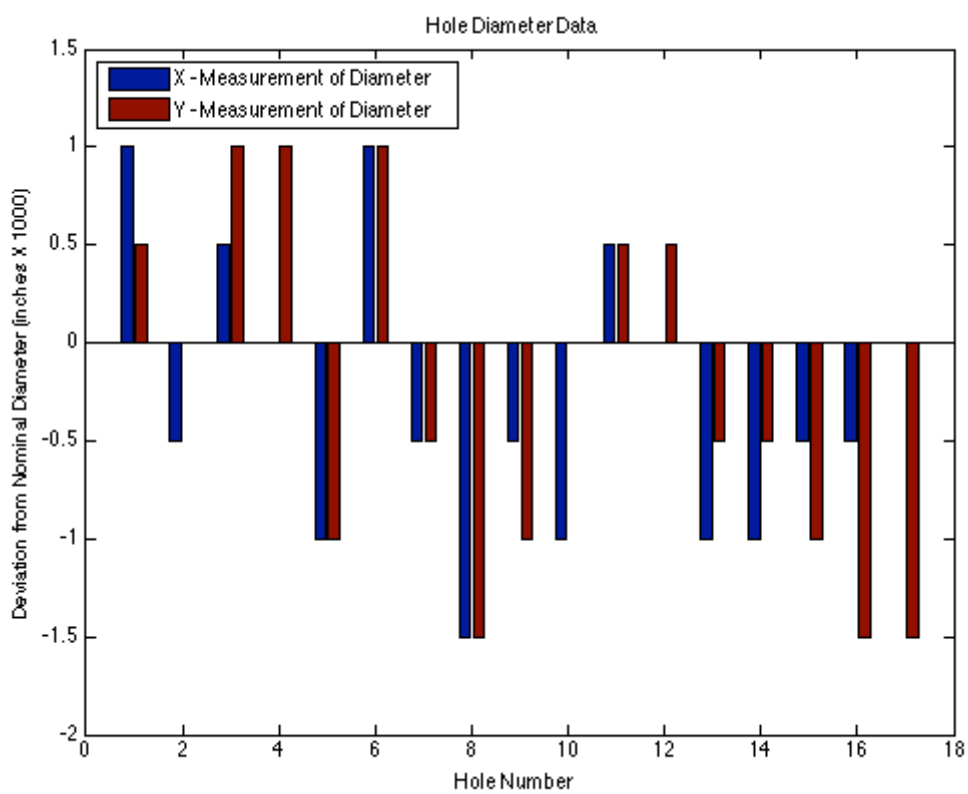
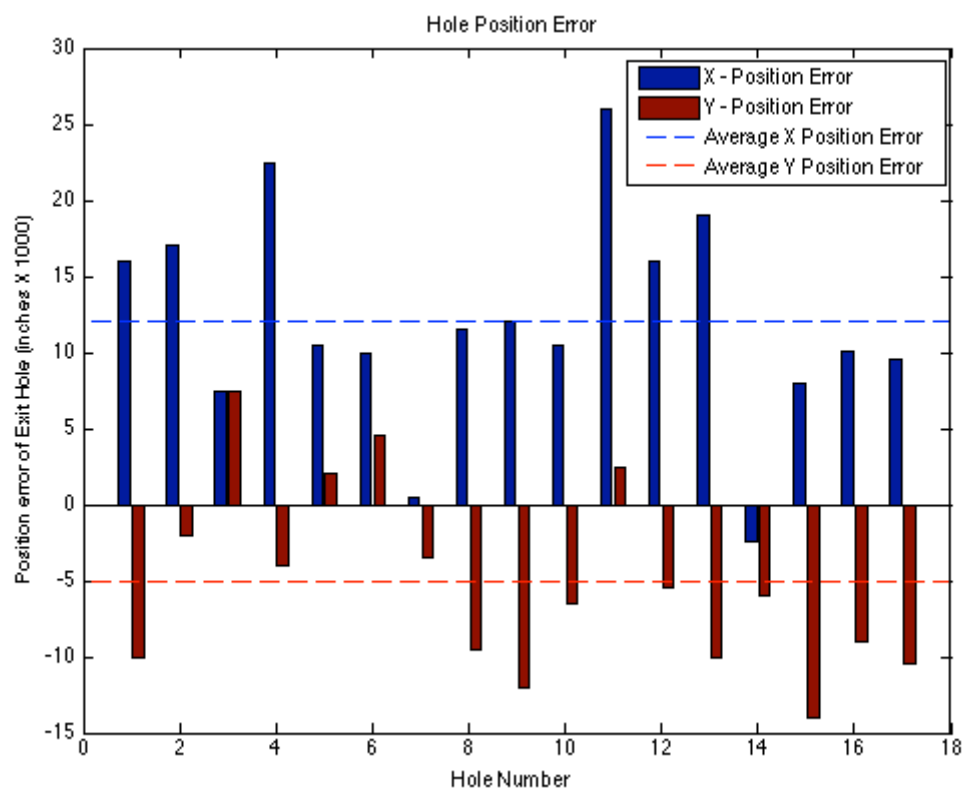
```
0.1270
```

```
MaxD =
```

```
0.1295
```

```
AvgD =
```

```
0.1282
```



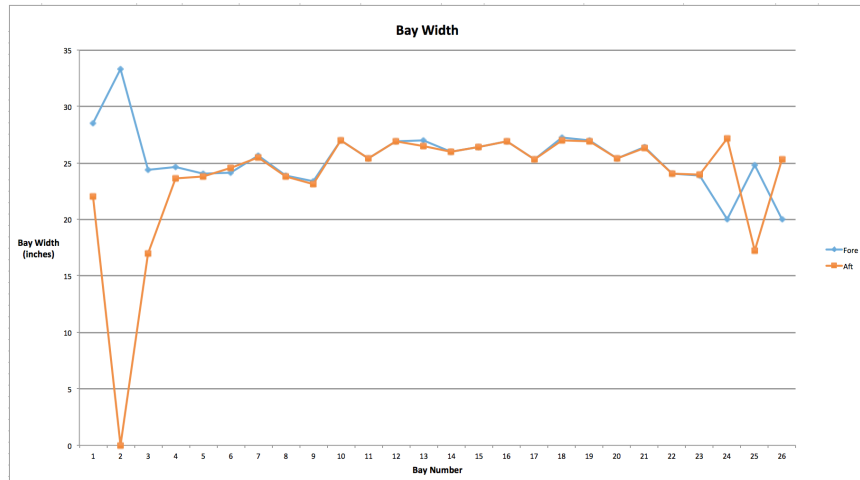


Figure A.1: This graph displays the width of each bay.

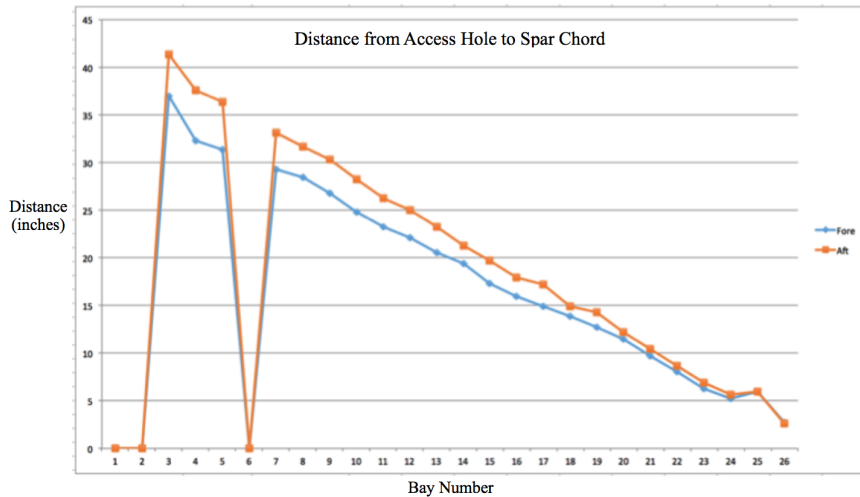


Figure A.2: This graph displays the length of each bay. This measurement represents the distance from the access hole in the center of the bay to the spar chord where back-drilling will be performed.

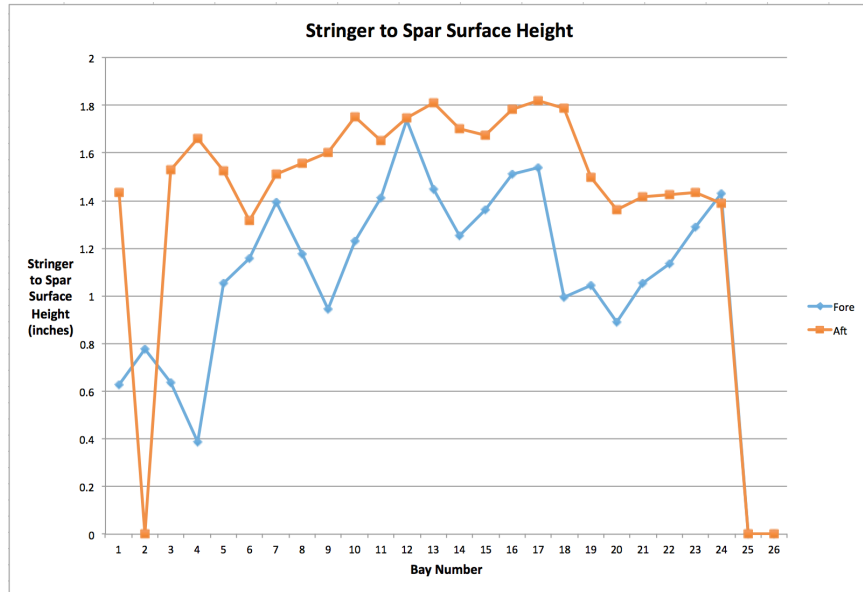


Figure A.3: This graph displays the height difference between the last stringer and the spar chord in each bay.

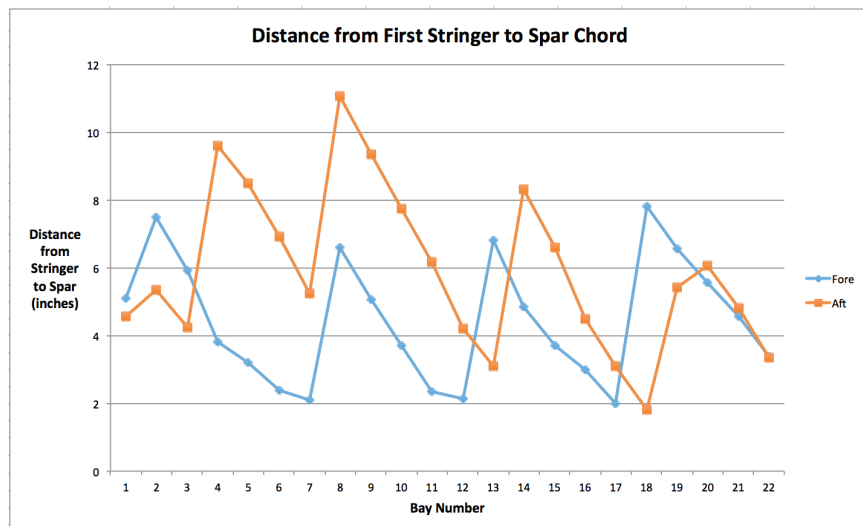


Figure A.4: This graph displays the horizontal distance from the last stringer and the spar chord in each bay.

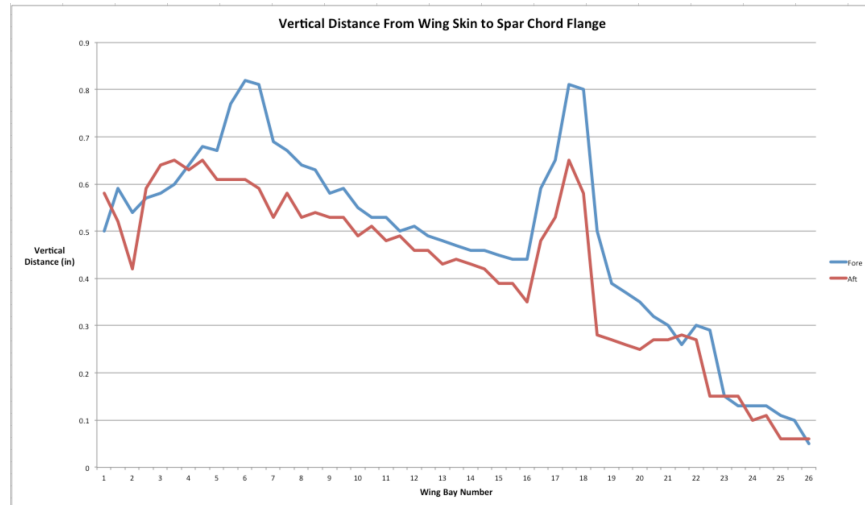


Figure A.5: This graph displays the height difference from the wing skin to the spar chord in each bay. Although the values range relative to each other, note that the absolute value is always less than an inch.

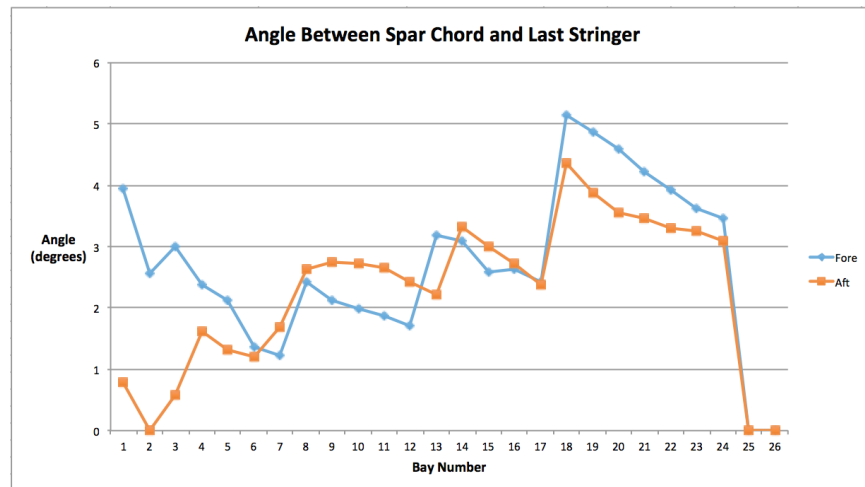


Figure A.6: This graph displays the angle between the last stringer and the spar chord for each bay. As can be seen, some of these values are near 5 degrees, which is significant. Fortunately, unlike the five-axis platform, the manually operated pneumatic tool is mounted directly to the wing skin and avoids these large angles.

	Group	Requirement	Baseline	Concept 2	Concept 3	Concept 4	Concept 5	Concept 6	Concept 7	Concept 8
Long Range Locomotion System			Human in the Box	Folding Tracked Crawler	Tank with turret on rails	Folding Rail system	Snake Arm system	Cable Robot	Continuous catapillar rails	Sloth crawler
	Spatial	Fits through hole		+	S	+	+	+	S	S
	Spatial	Height fits wing tip		-	-	-	+	-	-	-
	Time	Global more than 10 seconds		S	S	+	S	+	S	-
	Time	Initial bay setup		S	S	-	-	-	-	-
	Locomotion	Movement along rib		S	S	+	S	+	S	S
	Locomotion	Movement along spar		-	+	+	-	+	+	+
	Locomotion	Ease of reaching holes		-	-	-	-	-	-	-
	Stability	Stable end effector .01"		+	+	+	+	+	+	+
	Stability	No moment on stringers		S	S	S	S	S	S	S
	Operation	Cost		+	+	+	+	+	+	+
	Operation	Ease of use	Folding Tracked Crawler	S	+	+	-	-	S	S
	Operation	Ease of getting set up		+	+	-	+	-	+	+
	Operation	Umbilic and Cable Management								
	Operation	Controls	Folding Tracked Crawler	S	S	+	-	-	-	S
	Manufacturing	Complexity	Folding Tracked Crawler	S	S	S	-	+	-	S
			+	4	5	8	5	7	4	4
			-	3	2	4	6	6	5	4
			S	7	7	2	3	1	5	6
			Total	14	14	14	14	14	14	14
			Score	1	3	4	-1	1	-1	0

Figure A.7: This Pugh Chart analyzed the long range positioning system.

	Group	Requirement	Baseline	Concept 2	Concept 3	Concept 4	Concept 5	Concept 6	Concept 7
Local Locomotion System			Tank Turret with x-y-z axis	Centralized Robotic Arm	Moveable platform local end effector	Perimeter rail with single end effector	Turntable platform	Conveyor belt with end effector	Continuous catapillar rails
	Spatial	Fits through hole		+	+	+	S	+	+
	Spatial	Height fits wing tip		-	S	+	S	+	+
	Time	Local 10 seconds		-	S	S	S	S	S
	Time	Time b/t stops		S	-	S	S	S	+
	Time	Initial bay setup		S	-	S	S	S	S
	Locomotion	Movement b/t shear ties		-	-	S	S	S	+
	Locomotion	Movement along spar		-	S	S	S	S	-
	Locomotion	Ease of reaching holes		-	S	S	S	S	S
	Stability	Stable end effector .01"		-	S	S	S	S	S
	Stability	No moment on stringers		S	S	S	S	S	S
	Operation	Ease of use		-	S	S	S	S	S
	Operation	Ease of getting through hole and set up		+	-	S	S	S	S
	Operation	Umbilicle and Cable Management		S	S	S	S	S	S
	Operation	Controls		-	S	S	S	S	S
	Manufacturing	Easy to manufacture		-	S	-	S	-	-
	Manufacturing	Complexity		-	S	S	S	S	-
			+	2	1	2	0	2	4
			-	10	4	1	0	1	3
			S	4	11	13	16	13	9
			total	16	16	16	16	16	16
			Score	-8	-3	1	0	1	1

Figure A.8: This Pugh Chart analyzed the local positioning system, or arm design.

	Group	Requirement	Baseline	Concept 2	Concept 3	Concept 4	Concept 5
End Effector Y & X axis			Rack & Pinion	Ball Screw	Flex Track rack & pinion	Moving belt, stationary motor	Stationary belt, moving motor
	Spatial	Height		+	+	S	S
	Spatial	Width		S	S	S	S
	Spatial	Length constraints		-	S	-	-
	Time	Acceleration		S	S	+	+
	Stability	Precision		+	S	S	S
	Operation	Weight		-	+	+	+
	Operation	Controllability		+	S	+	+
	Manufacturing	Cost		+	-	+	+
	Manufacturing	Complexity		+	S	S	S
			+	5	2	4	4
			-	2	1	1	1
			S	2	6	4	4
			Total	9	9	9	9
			Score	3	1	3	3

Figure A.9: This Pugh Chart analyzed the various designs for an end-effector system.

## VITA

Benjamin Janicki is a graduate student researcher for the Boeing Advanced Research Center (BARC) at the University of Washington. He is completing his masters degree in Mechanical Engineering. His research for Boeing was on the development and design of confined-space automation systems for hole drilling applications in commercial airplane wings. This thesis describes his research work in detail.

Previously, he completed his undergraduate degree in Mechanical Engineering - also at the University of Washington. As an undergraduate he specialized in Mechatronics and graduated with Interdisciplinary Honors.

Benjamin Janicki is a native of the Pacific Northwest, having been raised in Mount Vernon, WA.

He welcomes your comments and questions at [benjaj2@uw.edu](mailto:benjaj2@uw.edu).